Two-dimensional distribution of living benthic foraminifera in anoxic sediment layers of an estuarine mudflat (Loire Estuary, France)

A. Thibault de Chanvalon[1,2], E. Metzger[1], A. Mouret[1], F. Cesbron[1], J. Knoery[2], E. Rozuel[2], P. Launeau[1], M. P. Nardelli[1], F.J. Jorissen[1], E. Geslin[1]

[1]{Université d'Angers, Université de Nantes, LPG-BIAF, UMR CNRS 6112, 49045 Angers Cedex, France }

[2]{Ifremer, LBCM, Rue de l'Ile d'Yeu, 44300 Nantes, France }

Correspondence to: A. Thibault de Chanvalon (athibaultdc@gmail.com, aubin.thibault-de-chanvalon@univ-nantes.fr)

Abstract

We present a new rapid and accurate protocol to simultaneously sample benthic living foraminifera in two dimensions in a centimetre scale vertical grid and dissolved iron and phosphorus in two dimensions at high resolution (200µm). Such an approach appears crucial for the study of foraminiferal ecology in highly dynamic and heterogeneous sedimentary systems, where dissolved iron shows a strong variability at a centimetre scale. On the studied intertidal mudflat of the Loire estuary, foraminiferal faunas are dominated by *Ammonia tepida,* which accounts for 92% of the living (CTG-labeled) assemblage. The vertical distribution shows a maximum density in the oxygenated 0-0.4 cm surface layer. A sharp decrease is observed in the next two centimetres, followed by a second well defined maximum in the suboxic sediment layer (3 - 8 cm depth). The presented method yields new information concerning the 2D distribution of living *A. tepida* in suboxic layers. First, the identification of recent burrows by visual observation of the sediment cross-section, and the burrowing activity as deduced from the dissolved iron spatial distribution show no direct relation with the distribution of *A. tepida* at a centimetre scale. This lack of relation appears contradictory to previous studies (Aller and Aller, 1986; Berkeley et al., 2007). Next, the heterogeneity of *A. tepida* in the 3-8 cm depth layer has been quantified by the Moran's Index to identify the scale of parameters controlling the *A. tepida* distribution. The results reveal horizontal patches with a characteristic length of 1 to 2 cm. These patches correspond to areas enriched in dissolved iron likely generated by anaerobic degradation of labile organic matter.

These results suggest that the routine application of our new sampling strategy could yield important new insights about foraminiferal life strategies, improving our understanding of the role of these organisms in coastal marine ecosystems.

1 Introduction

Intertidal estuarine mudflats are transitional areas between land and sea. This intermediate position explains the important horizontal, vertical (in the sediment column) and temporal heterogeneities in physical and chemical sediment properties. It also causes heterogeneous ecological niches with scales ranging from micro- to hectometres. When studying such heterogeneous environments, the observational scale has to be chosen as a function of the scale of the studied ecological niche variability (Wu et al., 2000; Morse et al., 2003; Martiny et al., 2006; Wu and Li, 2006). This is a fundamental prerequisite to further identify potential parameters controlling the heterogeneity of the niches.

Ecological studies of benthic foraminifera attempt to describe the main factors controlling foraminiferal communities, and their variability on different spatial and temporal scales (Buzas et al., 2015). The best described pattern concerns the spatial variability of their vertical distribution in open marine environments, on a hundred-kilometre scale. The conceptual model proposed by Jorissen et al. (1995) considers a regional variability of the spatial organization of foraminiferal taxa in the sediment column, where they occur in a succession of so-called microhabitats. The stratified succession of inhabited sediment layers is supposed to be a response to oxygen and organic matter availability, which changes vertically in the uppermost sediment, but also geographically, when going from oligotrophic (deep water, offshore) to eutrophic (shallow water, nearshore) conditions. In estuarine areas, on smaller scales, other major controls are invoked (e.g. emersion time, grain size, salinity), but they are less well documented. At a kilometre scale, the salinity, salinity variations and more generally the frequency of chemical exchanges with the ocean are often invoked as controls of foraminiferal assemblages (Debenay and Guillou, 2002; Debenay et al., 2006). Within the estuary, especially in cross-shore transects, emersion time seems to be a major controlling factor of species distribution at a decametre scale (Berkeley et al., 2007). But other parameters, such as grain size, pH or organic carbon lability could also have a significant impact. Estuarine foraminiferal faunas seem to show substantial patchiness at metre scale at

the sediment surface (Buzas, 1970; Hohenegger et al., 1989; Buzas et al., 2002, 2015). At a decimetre scale, the rare studies performed on intertidal mudflats highlight that grain size and topography could be important controls (Lynts, 1966; Morvan et al., 2006).

Finally, according to our knowledge, only three publications have analyzed the spatial surface organization at a centimetre scale, using an adequate sampling grid (Buzas, 1968 in Rehoboth Bay, Delaware; Olsson and Eriksson, 1974, on the Swedish coast; and de Nooijer, 2007 in the Wadden Sea). These three studies show that foraminiferal densities present a patchy distribution. Buzas (1968) hypothesized that this could be due to individual reproduction, leading to very localized and intermittent density maxima, so called "pulsating patches" (Buzas et al., 2015). Another field approach, at a centimetre scale, is to sample around inhabited burrows, using a non-regular sampling scale, by defining position, size and shape of each sample according to the burrow geometry. In this way Aller and Aller (1986) and Thomsen and Altenbach (1993) studied the foraminiferal distribution around macrofaunal burrows at subtidal stations and observed a threefold enrichment of foraminiferal density in the burrow walls. With a similar sampling strategy, Koller et al. (2006) showed a three hundred-fold enrichment of foraminiferal densities in the burrow walls of an intertidal station. These studies highlight the importance of macrofaunal activity at the centimetre scale as a potential control of foraminiferal spatial organization. They suggest the presence of oxic microenvironments around the burrows generated by bio-irrigation, attractive because of organic matter enrichment (Aller and Aller, 1986). Foraminifera could specifically colonize these environments favourable for aerobic respiration and therefore be found at depths below oxygen penetration.

However, another possible explanation for the presence of rich foraminiferal faunas in deeper anoxic layers could be the ability of some species to switch to alternative (*e.g.* anaerobic) metabolisms (Leutenegger and Hansen, 1979; Bernhard and Alve, 1996; Risgaard-Petersen et al., 2006; Heinz and Geslin, 2012). These two possible mechanisms lead to contrasted conclusions concerning ecological strategies. For example, a high density of living foraminifera along burrow walls compared to anoxic surrounding sediments may be explained by a positive response of the foraminiferal community to the availability of oxygen and labile organic matter (Aller and Aller, 1986; Loubere et al., 2011) or as the involuntary consequence of passive downward transport due to macrofaunal bioturbation followed by the development of a short term survival strategy based on a metabolism modification (Douglas, 1981; Alve

and Bernhard, 1995; Moodley et al., 1998). *In situ* distribution can answer this question by determining whether subsurface high density is only concomitant with burrows or whether living *A. tepida* are able to modify their metabolism in order to survive in suboxic environments (without both oxygen and sulphide) independently of burrows. Unfortunately, the sampling strategies used in the above mentioned references did not allow establishing the importance of burrows compared to other environmental physico-chemical parameters because the increased density observed in burrow walls was not compared to a "background heterogeneity" at the same scale. This precaution is necessary, especially when the increase of foraminiferal density is not at least of one order of magnitude. Consequently, a large uncertainty remains about the ubiquity and the nature of macrofauna-independent mechanisms that could cause foraminiferal heterogeneity.

The recent development of pore water sampling techniques with high resolution in two dimensions offers the advantage of providing simultaneously geochemical information on vertical and horizontal sub-millimetre scales (Stockdale et al., 2009; Santner et al., 2015). Several studies have evidenced important spatial variability of dissolved iron release into pore water (Jézéquel et al., 2007; Robertson et al., 2008; Zhu and Aller, 2012; Cesbron et al., 2014). This can be due to iron oxide consumption caused by local labile organic matter patches that favour anaerobic respiration (by dissimilatory bacteria; Lovley, 1991) or by enhancement of sulphide transport from the deeper layers through burrows and subsequent abiotic dissolution (Berner, 1970). Conversely, macrofaunal water renewal is also likely to bring oxic water into the burrows which consumes reduced dissolved iron and replenishes the stock of iron oxide. Direct burial of iron oxide by macrofauna may also contribute to the replenishment (Burdige, 2011). The overall role of macrofaunal activity on the sedimentary iron cycle is still unclear (Thibault de Chanvalon et al., in prep; Robertson et al., 2009). Phosphorus is also likely to have a heterogeneous geochemical pattern. Very marked centimetre scale patches were reported (Cesbron et al., 2014), apparently due to nutrient recycling from organic matter. However, iron oxide dissolution can also release adsorbed phosphorus according to a ratio up to P/Fe ~0.2 (based on ascorbate extractions; Anschutz et al., 1998) which can be compared to the theoretical anaerobic respiration ratio of P/Fe ~0.002 (Froelich et al., 1979). Using geochemical fingerprints, the combination of sub-millimetre resolution analyses of dissolved iron and phosphorus is thus likely to (1) confirm the burrow activity (iron oxidation) and (2) identify potential hotspots of organic matter consumption (phosphorus production independent to iron).

In the present paper, we present a new two dimensional sampling technique allowing first the investigation of the relation between benthic foraminifera and dissolved iron, and next, the analysis of the heterogeneity of foraminiferal distribution and then, the identification of the scale of potential controls such as active burrows or labile organic matter patches.

2 Material and methods

2.1 Site description

The Loire estuary (NW coast of France) is hyper-synchronous: it shows an increasing tidal range upstream (Le Floch, 1961) reaching a maximum spring tidal range of about 7m at 40 km from the mouth. At Donges (in the high tidal range area, right shore) the daily surface salinity range is about 20. Seasonally, surface salinity fluctuates from 0 during floods to 30 during low-water periods (network SYVEL, GIP Loire Estuaire). On the opposite shore, the largest mudflat of the estuary ("Les Brillantes", ~1350 ha) extends downstream from the city of Paimboeuf. During high tide, hydrodynamics (tide, wind induced waves, flow) constrains the sediment deposition/resuspension cycle whereas during low tide, biological factors (bioturbation, biofilm stabilization, benthic primary production; Round, 1964; Vader, 1964; Paterson, 1989) become more important and generate sediment burial and chemical transformations. Microphytobenthic biofilms vary annually between 20 mg m^{-2} in January and 60 mg m^{-2} in July (Benyoucef et al., 2014). Our sampling site (47°16'56.00"N 2° 3'47.00"W) is located on the slikke of "Les Brillantes" mudflat, below the Mean High Water Neap Tide level (MHWNT), about 20 m offshore from an active one metre high eroded cliff. Sediment is mainly composed of silt (92%) with some clay (6%) and sand (2%) (Benyoucef, 2014).

We sampled in May 2013, two weeks after a major flood (discharge volume at Paimboeuf >2500 $m^3.s^{-1}$, hydro.eaufrance.fr). During sampling, the river discharge was 835 m^3 s^{-1} on average. Air temperature was 12.7°C, the weather was cloudy and salinity in the surface waters of the main channel ranged from 0.6 to 20 (data from SYVEL network). Sediment samples were collected at the beginning of low tide. Porosity decreased from 0.917 to 0.825 in the first 5 cm (Thibault de Chanvalon et al., in prep). The calcite saturation state, calculated from alkalinity, sodium and calcium concentrations and pH (Millero, 1979, 1995; Mucci,

1983; Boudreau, 1996; Mucci et al., 2000; Hofmann et al., 2010) was above 1.0 until 9 cm depth (data not shown). The macrofauna was mainly composed of *Hediste diversicolor* (Annelida: Polychaeta, 630 ind m^{-2}) and *Scrobicularia plana* (Mollusca: Bivalvia, 70 ind m^{-2}) (I. Métais, personal communication, 2015).

2.2 1D sampling and processing

Four cylindrical cores (diameter 8.2 cm) were sampled using Plexiglas tubes. The first two cores were dedicated to foraminiferal analysis and were sliced immediately after sampling; every two millimetres from 0 to 2 cm and every half centimetre between 2 and 5 cm. Surface microtopography induces high uncertainty in the volume of the upper slice. Within one hour after retrieval, in order to distinguish living foraminifera, sediments were incubated with the staining molecule CellTracker Green™ in a final concentration of 1 µmol.L^{-1} in 50 mL of estuarine water for 10-19 hours (Bernhard et al., 2006). CellTracker Green is a non-fluorescent molecule, which is hydrolyzed by nonspecific esterases, producing a fluorescent compound. After incubation, samples were fixed in 3.8% Borax-buffered formalin and stored until analysis. In the laboratory, samples were sieved over 315, 150, 125 and 63 µm meshes, and the 150-315 µm fraction was examined using an epifluorescence stereomicroscope (i.e., 485-nm excitation, 520-nm emission; Olympus ZX12 with a fluorescent light source Olympus URFLT or Nikon SMZ 1500 with a PRIOR Lumen 200). All foraminifera that fluoresced continuously and brightly were wet picked, air dried, identified and counted.

The two other cores were used to constrain geochemistry. The first core was dedicated to microelectrode profiling and solid phase geochemistry. The solid phase was characterized by total organic carbon and reactive iron, manganese and phosphorus, extracted by an ascorbate reagent (buffered at pH 8) during 24 hours (Kostka and Luther III, 1995; Anschutz et al., 1998, 2005; Hyacinthe et al., 2001; Hyacinthe and Van Cappellen, 2004). See more details in Supplement (S1). Oxygen was analyzed with Clark's type electrodes (50µm tip diameter, Unisense©, Denmark) within the first 5 mm at a 100 µm vertical resolution. In the second core, Diffusive Equilibrium in Thin film in one dimension probes (DET 1D, adapted from Davison and Zhang, 1994; Krom et al., 1994) were incubated during one night for dissolved sodium, iron, manganese and phosphorus. Gel samples were eluted in HNO_3 0.01 M and

analyzed by ICP-AES. Salinity was estimated from sodium concentration. See more details in Supplement (S2).

2.3 2D sampling and processing

For the two-dimensional sampling, we used a "jaw device", composed of two main parts (jaws; Fig. 1). The first jaw is a DET gel probe, which samples the dissolved chemical species from the pore water at high resolution, whereas the second jaw samples a 2 cm-thick slice of the adjacent sediment, from which we sub-sampled 1 cm^3 aliquots for foraminiferal analysis. The first jaw is a 250 mm x 200 mm x 2 mm polycarbonate (Poly-methyl methacrylate**)** plate with a central depression of 1 mm that holds a 2D gel probe. The probe is made of two layers: 1) a 180 mm x 97 mm x 0.92 mm polyacrylamide thin-film prepared and rinsed with Milli-Q water (Krom et al., 1994) which reaches equilibrium in a few hours once incubated (called "2D DET gel") and 2) a PVDF porous (0.2 μm) membrane to protect the gel, prevent falling out the depression and control diffusion. The 2D DET gel was prepared and mounted less than one week before sampling, was conserved in a wet clean plastic bag and then, deaerated by N_2 bubbling for about 6h before deployment. The sampler was deployed into the sediment at low tide. On both lateral sides of the central depression (Fig. 1), plastic rails (2 cm high) were fixed in order to guide the second jaw to slide along the plate. The second jaw is a stainless steel plate (1.5 mm thick) bent on both sides. After equilibration (5h) of the 2D gel, the second jaw was inserted along the guides of the first jaw and the whole device was gently pulled out of the sediment. Once on shore, the 2D gel was separated from the sediment, covered with a plastic-coated aluminium plate and stored in an icebox with dry ice pellets (Cesbron et al., 2014), until final storage in a freezer (-18°C).

The sediment plate was manually cut (with stainless steel trowels) within 30 minutes in 1 cm^3 cubes for a surface of 8 cm x 8 cm. The resulting sampling map is presented in Fig. 2 together with the 1D sampling scheme of foraminifera. Next, these sediment cubes were labelled with CTG to recognize living foraminifera (as for the core slices, see 2.2). Considering an error of 1 mm for each cut, the volume uncertainty was ~14%, except for surface samples where the microtopography of the sediment surface considerably increases volume uncertainty.

The 2D DET probe was analyzed in order to obtain the concentrations of dissolved iron and dissolved reactive phosphate (DRP) (Cesbron et al., 2014). Quickly, after thawing at ambient temperature, the sample gel was recovered by a reactive gel equilibrated in specific colorimetric reagents. Twenty five minutes after contact, a photograph (reflectance analysis) of superposed gels was taken with a hyperspectral camera (HySpex VNIR 1600) and analyzed (see 6.3 for more details). The resolution (surface area of pixels) was 211 µm x 216 µm. The estimated incertitude is 10% for iron and 11% for DRP. See more details in Supplement (S3). To compare the geochemical species distribution (at submillimetre resolution) and foraminiferal density (at centimetre resolution), a handmade R code was written allowing the downscaling of chemical resolution from 0.2 mm to 1 cm.

2.4 Statistical analyses

Patchiness effect or autocorrelation, interpreted as the fact that the density of one square depends on its neighbours, was explored using spatial correlograms built using Moran's Index (I), computed with R (package "spdep" following (Fortin and Dale, 2005; Bivand et al., 2008; Legendre and Fortin, 2010; Borcard et al., 2011), equation (1)). This index was applied to benthic meiofauna by Blanchard (1990) and Eckman and Thistle (1988) and to foraminifera by Hohenegger et al. (1993). This index calculates the similarity of pair values for one neighbourhood, a neighbourhood being defined by a weight ($w_{i,j}$) function of the distance (d) between pairs.

$$I(d) = \frac{\sum_{i,j}^{n} w_{i,j}(d)(x_i-\bar{x})(x_j-\bar{x})}{\sqrt{\sum_{i}^{n}(x_i-\bar{x})^2}} \times \frac{n}{\sum_{i,j}^{n} w_{i,j}(d)} \quad (1)$$

Here, the n = 40 cubes used for Moran's Index have neighbourhoods defined as cubes in direct contact (4 neighbours per sample with a weight of 1, others have 0, also known as "rook connectivity"; Fortin and Dale, 2005). With this configuration, Moran's Index is -1 for a contrasted organization (perfect negative correlation between neighbours) and +1 in case of grouped organization (perfect positive correlation between neighbours). A value close to zero ($I_0=(n-1)^{-1}$) corresponds to no organization or random distribution. The correlogram plots Moran's Index versus the order of the neighbours (o.n.). A decrease of the Moran's Index from positive to negative values characterizes a patchy distribution. The characteristic length of the patchiness is defined as the order of neighbours when $I_{o.n.}=0$ (Legendre and Fortin, 1989). Two dimensional non-random organization has been tested with the alternative

hypothesis: $I_{o.n.}>I_0$. The second test examines if there is a preferential direction in the organization (isotropy). Again, the alternative hypothesis $I_{o.n.}>I_0$ for Moran's Index is used, restricting the distance to the tested dimension (vertical or horizontal). Thus, in our case, each sample was compared only with its lateral or vertical neighbours (i.e., 2 neighbours per test).

3 Results

3.1 1D geochemical features

Figure 3 shows both solid and dissolved chemical species obtained from the dedicated cores. Total organic carbon (C_{org}, black circles, Fig. 3A) decreased from 2700 µmol g(dry sed)$^{-1}$ to 1900 µmol g(dry sed)$^{-1}$ in the first centimetre, then increased sharply until 1.5 cm depth, and finally decreased progressively from 2700 µmol g(dry sed)$^{-1}$ to 2400 µmol g(dry sed)$^{-1}$ at 5 cm depth. Salinity (Fig. 3A) ranges from 7.5 to 1.7 with an offset of ~2 between replicates and a decrease of ~3 in the 13 first centimetres. Figure 3B shows the vertical distribution of dissolved oxygen. The three profiles shown (out of 18) are considered representative of the lateral variability in the sediment. Most of the oxygen concentration profiles show the exponential trend typical for undisturbed marine sediments (2 profiles in Fig. 3B, with light grey and white diamonds; Revsbech et al., 1980; Berg et al., 1998). However, one third of the O_2 profiles diverged from the exponential model, showing an interruption of the decreasing trend, or even a local increase, at depth (e.g. the profile with dark grey diamonds represented in Fig. 3B). The Oxygen Penetration Depth (OPD) remained relatively constant around 2.0 mm (sd=0.2 mm, n=18) despite this heterogeneity.

Figures 3C, 3D and 3E show the distribution of manganese, iron and phosphorus, respectively, both in the dissolved phase (grey and open diamonds) and in the easily reducible solid phases (black circles, extracted by ascorbate leaching (Anschutz et al., 2005; Hyacinthe et al., 2006)). Extracted manganese (mainly (hydr)oxide, black circles in Fig. 3C) showed a strong enrichment of the easily reducible solid phase (until 13 µmol g(dry sed)$^{-1}$) in the first two millimetres, where an important upward diminution was visible in both replicates of the dissolved phase (grey and open diamonds in Fig. 3C). Below, the solid phase showed a slightly decrease from 7.9 to 5.6 µmol g(dry sed)$^{-1}$ until 5 cm depth. The dissolved manganese concentration decreased between 4 and 9 cm depth in both replicates (from 70 to 30 µmol L^{-1}). In the solid phase, iron, phosphorus and manganese are strongly correlated when the surface sample is not considered (r^2=0.70 and 0.55 between iron and manganese, and iron and

297 phosphorus, respectively). Profiles of dissolved iron and phosphorus are also strongly
298 correlated (r^2=0.90, slope=1.87 and r^2=0.47, slope=1.31 for replicates A and B). Iron and
299 phosphorus were remobilized, and therefore appeared in the dissolved phase, between 1 and 9
300 cm. Both replicates of dissolved iron showed the same four well described maxima (at least
301 six samples for each maximum) at 2.3, 3.3, 5.9 and 7.3 cm depth but with different
302 concentrations. In replicate A (open diamonds) these maxima have five times higher iron
303 concentrations (up to 700 µmol L^{-1}) than in replicate B.
304

305 **3.2 Visual features on the sediment plate**

306

307 Figure 4A shows the sediment slice obtained from the "jaw device" facing the 2D DET gel. In
308 order to facilitate the description, the figures were subdivided in centimetre squares labelled
309 with letters for the horizontal position and numbers for the vertical position. The black
310 rectangle corresponds to the 2D DET gel position, the blue rectangle to the gel signal
311 exploited and the red rectangle to the 2D foraminiferal sampling. Burrows parallel to the
312 cutting plan are visible over their entire length. When perpendicular to the cutting plan, they
313 appear as a dark hole (B14 in Fig. 4A). Figure 4B summarizes burrow distributions
314 superimposed on a picture of the gel after equilibration with the colorimetric reagents (pink
315 coloration corresponds to iron and blue to dissolved reactive phosphorus (DRP)). Five
316 burrows were visibly connected to the sediment surface; their traces mostly extended
317 vertically down to 10 cm depth where their track is lost. Between 10 and 15 cm depth, visible
318 burrow density decreased. Below 15 cm depth, burrows were rarely observed and the
319 sediment was dark (Fig. 4A). During slicing of the sediment plate, living polychaetes (*Hediste*
320 *diversicolor*) were observed in some burrows.
321

322 **3.3 2D DET gel**

323

324 Figure 5 shows the 2-dimensional datasets, with the distribution of dissolved phosphorus (Fig.
325 5A) and iron (Fig.5B) obtained from the 2D DET gel. For comparison, burrow distribution is
326 shown in Fig. 5A. Dissolved iron and phosphorus both appeared a few millimetres below the
327 sediment-water interface. They are positively correlated for the whole plate (r^2= 0.59,
328 slope=2.7). Despite their patchy distribution, both species can be observed along the entire
329 length of the gel probe (i.e. 17 cm depth). A main feature was the occurrence of two

prominent vertical structures enriched in dissolved iron and phosphorus (A-B/6-9 and F-G/5-14). The highest concentrations, of about 170 and 50 µmol L^{-1} for iron and phosphorus, respectively, were found within the structure at the right (squares F/8-9). In the structure at the left (A/6-8), iron and phosphorus maxima were around 120 and 25 µmol L^{-1}, respectively.

Most burrows seem to impact the iron concentration. For example, burrows 1, 3 and 5 clearly correspond (in the 4 first centimetres) to a drastic decrease or even disappearance of dissolved iron, whereas other burrows seem to correspond to a dissolved iron enrichment (F-G/5-9). However, some centimetre size patches (e.g. A-B/6-9, H-G/8-9 and F-G/17) seem to be unrelated to burrow structures. Below 15 cm depth, the sediment was dark and dissolved iron generally decreased whereas DRP increased.

3.4 Living foraminiferal distribution

Figure 5C shows the distribution of CTG-labelled *Ammonia tepida* determined for $1cm^3$ samples in the sediment facing the 2D DET gel. The analysis of living foraminifera in the 64 cubes (8 cm width * 8 cm depth) takes roughly the same time as the analysis of one core of 8.2 cm of diameter (until 5 cm depth). *Ammonia tepida* was by far the dominant species, accounting for 92% of the total assemblage. The second most frequent species, *Haynesina germanica,* represented 5% but its low density (mostly 0, 1 or 2 individuals per cubic centimetre) was not sufficient to support a reliable discussion. For this reason the data relative to this species are omitted from the present paper. *A. tepida* density ranged from 0 to 38 ind cm^{-3} with important lateral and vertical variability. The relative standard deviation (rsd) calculated for each raw is, on average, 45%, whereas for each column the rsd is 60%, suggesting a slightly more pronounced vertical organization. This is confirmed by the stratification of the richest samples (≥27 ind cm^{-3}) which were found in the topmost cm and below 6 cm depth, whereas the poorest samples (≤ 5 ind cm^{-3}) were found between 1 and 3 cm depth. Each row from the 2D distribution can be represented by a whisker plot (Fig. 6). The results confirm a three-step pattern with high densities at the surface (13 to 38 ind. cm^{-3}), lower density between 1 and 3 cm depth (0 to 12 ind cm^{-3} and one outlier at 24 ind. cm^{-3}) and increasing values below 3 cm (7 to 31 ind cm^{-3}).

This vertical pattern is also visible in the two studied sediment cores (Fig. 6): high densities of *A. tepida* (26 ± 0 ind. cm^{-3}) are observed in the first 2 mm, a rapid decrease to minimal densities in the 1.0 - 1.2 cm layer (3 ± 0 ind. cm^{-3}), followed by a progressive, somewhat irregular increase until 9 ± 0 ind. cm^{-3} below 2 cm depth to 8cm depth. Despite the different vertical sampling resolution, the densities observed in the cores are in agreement with the average densities observed in the sediment slice cubic samples.

4 Discussion

4.1 A methodological improvement to characterize heterogeneity

Here, we present for the first time a methodology allowing the simultaneous study of the vertical and horizontal heterogeneity of dissolved chemical species and living foraminifera (determined by CTG labelled) in the 8 first centimetres of the sediment. Figure 6 compares the vertical density distribution of *A. tepida* between the cores (triangles) and the jaw device (whisker plots), sampled a few decimetres apart. Despite the different vertical sampling resolution, the densities observed in the cores (sampling surface of 53 cm^2) are in agreement with the average densities observed in the sediment slice samples (sampled with the "jaw device", sampling surface of 8 cm^2). This similarity suggests a limited horizontal heterogeneity of *A. tepida* at a decimetre scale, although it is impossible to draw firm conclusions on the basis of only three samples (the two cores and the jaw device).

The jaw device (boxplot whiskers, Fig. 6) reveals a heterogeneous horizontal distribution at the centimetre scale. The centimetre scale heterogeneity is quantified by calculating the Moran's Index that estimates the characteristic length of foraminiferal niches. Figure 7 shows the Moran's Index correlograms applied between 3 and 8 cm depth (suboxic sediment) where high densities of living foraminifera were observed. Figure 7A shows that the spatial organization of *A. tepida* is patchy at a centimetre scale (I_1=0.24, p-value=0.013). For farther neighbours the Moran's Index values drop to zero, describing a random organization. Concerning vertical and horizontal heterogeneities, Moran's index values for direct neighbours are 0.02 and 0.47, with p-values of 0.38 and 0.001, respectively. For second order neighbours, values do not significantly differ from 0 in either direction (data not shown). This means that *A. tepida* specimens tend to be grouped in horizontal spots with a characteristic length of 1 to 2 cm.

Figure 7B shows the Moran's Index correlogram for iron at 1cm scale resolution (phosphorus is similar and not shown). It shows strong patchiness (I_1=0.7) for direct neighbours in either directions, with a characteristic length of 3-4 cm. The fact that the characteristic lengths of *A. tepida* (Fig. 7A) and dissolved iron (Fig. 7B) patches are longer than 1 cm suggests that the impact of different sampling thicknesses (roughly null for dissolved iron against 1 cm for foraminifera) would not result in major bias. Moreover, this characteristic length is important

as it likely corresponds to the characteristic length of the controlling mechanisms (Clark, 1985; Wu and Li, 2006). In fact, the difference in Moran's Index between chemical species and the *A. tepida* density distribution suggests that not exactly the same mechanisms control these parameters. This is an unexpected result, since most conceptual models explain benthic foraminiferal distribution in the sediment as a direct response to geochemical gradients, especially oxygen and sulphide (Jorissen et al., 1998; Van der Zwaan et al., 1999; Fontanier et al., 2002; Langezaal et al., 2006; Langlet et al., 2013), that intimately control iron remobilization.

4.2 Factors generating chemical heterogeneity

The heterogeneity of geochemical patterns is mainly explained by the availability of oxidants mineralizing organic carbon. In the generally applied conceptual model of Froelich et al., (1979), organic matter remineralization is characterized by a succession of horizontal layers where specific oxidants are used. Figure 3 confirms this theoretical vertical stratification: oxygen is rapidly consumed by respiration (about 2 mm depth, Fig. 3B); next, reduced dissolved manganese appears (Fig. 3C). Dissolved iron appears still deeper, with a first maximum at 2 cm depth. The slopes of the concentration profiles are steeper and the reactive solid phase (Figs. 3D and 3C) is more concentrated for iron than for manganese, suggesting a higher reactivity. However, the strictly vertical succession of redox layers is no longer respected in the deeper suboxic layers, as suggested by the presence of multiple maxima of iron (Fig. 3D) and by the high lateral heterogeneity observed in Figs. 5A and 5C. This high lateral heterogeneity cannot be explained by vertical diffusion of oxygen. It appears therefore that a strictly vertical stratification of redox zones, defining a similar foraminiferal microhabitat succession, is not a reasonable assumption, in our study area.

4.2.1 Macrofaunal impact on heterogeneity

Macrofauna is assumed to be the most important cause of chemical heterogeneity at a scale of 0.01cm (roughly the foraminiferal scale) to 100 cm (station scale), because of its ability to reorganize the sediment. In this way, macrofauna determines whether other factors can impact the heterogeneity of dissolved iron and/or *A. tepida*. Macrofauna modifies: i) the sediment texture/composition (burrow walls or fecal pellets); ii) the redox conditions, by ventilation of

their burrows with oxygenated water (bioirrigation) and iii) particle arrangement, by crawling or burrowing (biomixing) (Meysman et al., 2006). The efficiency of biomixing to homogenize the sediment mainly depends on two aspects (see Wheatcroft et al., 1990; Meysman et al., 2010a for a more detailed discussion):

(1) the biomixing species assemblage. At the "Les Brillantes" mudflat, the main macrofaunal species are *Hediste diversicolor* (630 ind m^{-2}) and *Scrobicularia plana* (70 ind m^{-2}, I. Métais, personal communication, 2015). *H. diversicolor* is a gallery-diffusor (particle mixing due to burrowing activity) whereas *S. plana* is an epifaunal biodiffusor (particles are mixed in a random way over short distances along the surface (e.g., François et al., 2002; Kristensen et al., 2012). These two species generate homogeneity or heterogeneity according to the second criterion. See below.

(2) the relation between the average time of existence of the studied objects (here foraminifera and dissolved iron) in the bioturbated area and the average time between two bioturbation events. Frequent bioturbation events generate efficient mixing (homogeneity) whereas rare bioturbation events generate heterogeneity. The average time between two bioturbation events is estimated to days to months by tracer modelling (Wheatcroft et al., 1990; Meysman et al., 2003, 2008) while the longevity of foraminifera in suboxic environments is estimated to roughly one year (Langlet et al., 2013; Nardelli et al., 2014). The mean residence time of iron in the dissolved phase is estimated between 2 and 3 days (Thibault de Chanvalon et al., in prep). Therefore, biomixing should generate a homogeneous distribution of foraminiferal density distribution, contrasting with a heterogeneous distribution of dissolved iron (and DRP). The different timespans also suggest that most of the living foraminifera were already present in the suboxic sediment before the visible (most recent) burrows were created. Conversely, the heterogeneity of the dissolved chemical species should be directly related to biomixing and to others factors that have not been homogenised by biomixing *i. e.* with a short time of existence in suboxic environments.

4.2.2 Geochemical impact of biogenic factors

The factors likely to generate chemical heterogeneity are : (1) Bioirrigation, that mainly causes an increase of oxidant availability (Aller and Aller, 1986; Aller, 2004; Arndt et al., 2013), and (2) Biogenic particles (e.g. decaying macrofauna, fecal pellets), that cause an increase of labile carbon availability. Dissolved iron shows two opposite types of behaviour

(Aller, 1982): (1) iron precipitates as a hydroxide when the oxidative state of the pore water surrounding active burrows increases (Meyers et al., 1987; Zorn et al., 2006; Meysman et al., 2010b). This is confirmed by visible burrows in Fig. 5 in which both dissolved iron and DRP are depleted (Figs 4, numbers 1, 3, 5 (above 6cm depth) and burrows in B-C-D13, E9-11,G-H10-15 and A-B9). These structures are mainly vertical and have a length often exceeding 3 cm, in agreement with the Moran's Index correlogram. Conversely, within the long burrow F-G/5-9, dissolved iron is enriched, indicating that this burrow is abandoned and no oxygen renewal occurs. This feature was also observed for some burrows by Zhu and Aller (2012) and Cesbron et al. (2014). (2) Dissolved iron is produced by anaerobic respiration where biogenic particles increase labile carbon availability, and thereby decrease the oxidative state of surrounding pore waters (Robertson et al., 2009; Stockdale et al., 2010). The geometry and isolation from visible burrows of patches A/7-8, G-H/8-9 and F-G17 in Figs. 5A and 5B suggest that they could represent centimetre-wide labile organic matter patches. We hypothesize that these patches correspond to intense remineralization of biogenic particles that dissolves iron oxides.

4.3 Mechanisms controlling the *A. tepida* distribution

The Figs. 5C and 6 clearly describes a three-step pattern in the distribution of *A. tepida*, with high densities at the surface, low densities between 1 and 3 cm depth and a somewhat surprising increase below (in suboxic sediments). A similar pattern was reported, but not discussed, for other intertidal environments (Alve and Murray, 2001; Bouchet et al., 2009). In our study, the consistency of the 8 vertical columns from the plate sampling confirms the robustness of this pattern and the two dimensional approach reveals an organization of *A.tepida* in centimetre-wide patches in the suboxic sediment. The next subchapters discuss possible mechanisms that could explain these features, especially in the suboxic environment where active burrows (supporting biomixing and bioirrigation) and biogenic particles have been identified as factors likely to generate such heterogeneity. .

4.3.1 Foraminiferal metabolism

Generally, aerobic metabolism is considered as the dominant mechanism in oxic conditions since it is energetically most efficient. In fact, Figs. 5C and 6 clearly describe maximal

densities of *A. tepida* at the sediment surface (0-2 mm depth) and low densities below (6-18 mm depth). This strong gradient of *A. tepida* density highlights the presence of a continuously oxygenated microhabitat enriched in organic matter (see TOC and O_2 profiles, Fig. 3A-B) close to the sediment-water interface, favourable for *A. tepida*. Energetic considerations and some observations that report a strong seasonal variability in the oxic zone (Moodley, 1990; Barmawidjaja et al., 1992), led to assume that foraminifera reproduce preferentially in the oxic layer (de Stigter et al., 1999; Berkeley et al., 2007). Together, these factors explain the maximum density in the surface layer.

Since the work of Richter (1961), numerous publications have reported living benthic foraminifera in suboxic sediment layers(Jorissen et al., 1992; Moodley and Hess, 1992; Bernhard and Sen Gupta, 2003). For intertidal environments, studies have reported living (Rose Bengal stain) foraminifera in subsurface environments since the 1960's (*e. g.* Buzas, 1965, Steineck and Bergstein, 1979). Several *in situ* (Goldstein et al., 1995; Bouchet et al., 2009) and laboratory studies (Moodley and Hess, 1992; Moodley et al., 1998; Pucci et al., 2009; Nardelli et al., 2014; Nomaki et al., 2014) with *A. tepida* also reported survival, activity and even calcification in suboxic conditions. Anaerobic metabolism would be a logical mechanism to explain the presence of large amounts of living foraminifera in suboxic layers. Complete or partial (with endo and/or ectobionts; Bernhard and Alve, 1996) denitrification co-occurring with nitrate storage has been demonstrated for some foraminiferal taxa (Risgaard-Petersen et al., 2006). Nomaki et al., (2014) have suggested denitrification by endobionts for *A. tepida*. However, denitrification has not been measured in *A. tepida*, and only very low intracellular nitrate concentrations were found (Pina-Ochoa et al., 2010; Geslin et al., 2014). It appears therefore unlikely that the abundance of living *A.tepida* in deeper suboxic layers can be explained by active colonization.

4.3.2 Burying and burrow microenvironment

It is clear that biomixing is a likely mechanism to explain the introduction of foraminifera in deeper sediment layers, by passive transport (Alve and Bernhard, 1995; Goldstein et al., 1995; Moodley et al., 1998; Saffert and Thomas, 1998; Alve and Murray, 2001; Jorissen, 2003). However, the spatial distribution resulting from this passive transport has never been well described, or modelled. According to the theory of biomixing, we suggest that the vertical distribution of *A. tepida* can be approached by a diffusion model, which should lead to an

exponential downward decrease, with the slope as a function of the mortality rate. Possibly, *A. tepida* is able to survive in suboxic environments using an intermittent aerobic metabolism, using the oxygen that can be punctually available due to bioirrigation (Fenchel, 1996; Wang et al., 2001; Wenzhofer and Glud, 2004; Pischedda et al., 2012). Their activity should progressively decrease once oxygen is depleted; (Phipps, 2012) suggested that they could finally be immobilized before dying in case of a prolonged absence of oxygen supply. We think that repeated introductions by macrofaunal bioturbation, followed by reduced metabolic activity, leading to immobilisation, is the most likely mechanism to explain the high abundances of living foraminifera in suboxic sediments.

Figures 4A and 5B show no relation between visible burrows and living *A. tepida.* This result is in agreement with the different time-scales of the foraminiferal lifespan and the burrows, and with the idea that biomixing homogenizes the *A. tepida* density. It suggests also that the oxygenation obviously generated by formation of new burrows is consumed too fast to allow all infaunal *A. tepida* to migrate to these active burrows. Thus, recent burrow walls are apparently not colonized by specimens of *A. tepida* already present in the suboxic sediment. Our observations contrast with earlier studies, showing increased foraminiferal densities (up to 300 times higher than in the surrounding sediment, rose Bengal staining) in burrow walls. For example, data from burrows of *Amphicteis* sp. at 4800m depth (Aller and Aller, 1986), of *Echiurus echiurus* at 42m depth (Thomsen and Altenbach, 1993) and of *Pestarella tyrrhena* in intertidal sandflats (Koller et al., 2006) all presented high foraminiferal densities. The observed differences could be due to the fact that burrows of various macrofaunal taxa may represent very different environmental conditions and eventually due to a difference in sampling scale, since Thomsen and Altenbach (1993) and Koller et al. (2006) applied an irregular millimetre sampling around burrows. Summarizing, macrofaunal activity would explain transport to and survival in suboxic layers. However, it does not explain the density minimum at 1-3 cm depth.

4.3.3 Sensitivity to geochemical gradients

We think that the most probable explanation for the 1-3 cm density minimum of *A. tepida* is an active upward migration of the specimens, back to the sediment surface, before they are completely immobilized by a lack of oxygen and a strongly lowered metabolism. Numerous

studies have already reported that vertical migration of foraminifera allows them to move to more hospitable environments (Jorissen, 1988; Van der Zwaan and Jorissen, 1991; Alve and Bernhard, 1995; Moodley et al., 1998; Gross, 2000; Langezaal et al., 2003; Geslin et al., 2004; Ernst et al., 2005). In an experiment in which populations of *Haynesina germanica* were uniformly mixed in a 6 cm sediment column, Ernst et al. (2006) saw a clear migration back to the surface for the foraminifera living between 1 and 3 cm depth, and suggested that foraminifera living at greater depth were unable to do so. Similarly, Hess et al. (2013) showed that benthic foraminifera are able to migrate through suboxic sediment to reach oxic sediments over a maximal distance of a few centimetres. Active migration towards directly detected oxygen or organic matter over distances beyond 1 cm seems improbable, since this distance is much higher than the typical pseudopodial length (about 1 cm, see Travis and Rabalais, 1991). However, as described above, the presence of oxygen could be indirectly detected by other geochemical gradient (e.g. NO_3^-, Mn^{2+} or Fe^{2+}, dissolved organic carbon, pCO_2). However, when gradients generated by the oxygen front are imperceptible for *A. tepida*, because they are living too deep in the sediment, or when such gradients are hidden by other sources of geochemical gradients (as organic-rich patches), this upward migration could no longer occur. This could explain why below 3 cm depth, *A. tepida* remains in the deeper sediment layer after being transported there accidentally.

However, the organization of the foraminiferal in 1 to 2 cm-wide horizontal patches identified by Moran's Index suggests that *A. tepida* detects not only vertical geochemical gradients, but probably also lateral gradients around degrading biogenic particles. The characteristic length of patches corresponding to biogenic particles identified by dissolved iron maxima (A/7-8, G-H/8-9 and F-G17 in Fig. 7C and 7D, see 4.2.2) is in agreement with the characteristic length of foraminiferal density maxima. For instance, in the 8 first centimetres, the two identified biogenic particles patches (A/7-8, G-H/8-9 in Fig. 5B) both correspond to a higher density of *A. tepida* (28/19 and 21/30 ind cm^{-3} in average for A/7-8 and G-H/8 respectively, Fig. 5C). In agreement with these results and despite a lowered metabolism, we hypothesize that foraminifera could move towards patches of labile organic matter even in deeper suboxic layers. Nevertheless, a better identification of labile carbon patches, replicate sampling with the here developed strategy and experimental studies with artificial geochemical gradients are necessary to confirm our hypotheses about the behaviour of *A. tepida* in suboxic environments.

Summarizing, we suggest that the distribution of *A. tepida* can be interpreted as the result of not less than five interacting mechanisms (Fig.8). 1) high foraminiferal densities at the surface are the result of the presence of abundant labile organic matter and reproduction in the oxygenated layer (§4.3.1), 2) downward transport by macrofaunal biomixing introduces living foraminifera in deeper sediment layers (§4.3.2), 3) in the 3 first centimetres foraminifera are capable to migrate back to the oxygenated, organic-rich surface layers once they detect redox gradients, whereas in deeper sediment layers, they are no longer capable to find their way back to the superficial oxygenated layer (§4.3.3), 4) after a prolonged presence in suboxic conditions, foraminifera lower their metabolism and become inactive, 5) foraminifera can be temporarily re-mobilized during intermittent bioirrigation events, and can eventually migrate towards organic-rich microenvironments in their vicinity (§4.3.3). A better identification of labile carbon patches, for example based on alkalinity (Bennett et al., 2015), pCO_2 (Zhu et al., 2006; Zhu and Aller, 2010) or dissolved organic carbon should permit to go further in the interpretation.

5 Conclusion

We present a new, simple and robust sampling protocol, to obtain the 2D distribution of benthic foraminifera combined with the 2D distribution of geochemical species, here dissolved iron and phosphorus. This technique allows visual observation of burrow features. Geochemical features allowed us to recognise active burrows (with minimal dissolved concentrations), and to determine that areas of dissolved iron and phosphorus enrichment do not always represent abandoned burrows. Our observations on an estuarine mudflat showed an important density of *A. tepida* in suboxic environments with a characteristic length of patches of 1 to 2 cm. Surprisingly, no direct relation was found between active burrows and the *A. tepida* distribution. However, an enrichment of *A.tepida* was observed in some areas where dissimilatory iron reduction was intense; suggesting that even in suboxic environments, there is a relation between the spatial distribution of *A. tepida* and labile organic matter remineralisation. Our results show that the new sampling strategy proposed here can yield important new insights in the functioning of suboxic environments in estuarine mudflats.

6 Supplementary materials

S1 Solid geochemistry

The two cores were used to constrain geochemistry. They were stored at *in situ* temperature until processing, and were processed in a field laboratory. The first core was dedicated to solid phase geochemistry and microelectrode profiling (see section 2.2.3). The solid phase was characterized by total organic carbon, reactive iron, manganese and phosphorus. After profiling, the core was sub-sampled using a tube of 3 cm diameter and sliced every 2 mm until 2 cm and every 5 mm until 5 cm depth (Fig 2 A). After slicing, samples were immediately frozen with carbonic ice. Within a week, sampled were freeze-dried, the weight difference before and after freeze-drying served to calculate porosity. Next, samples were manually ground using an agate mortar and separated into two aliquots for chemical analyses.

The first aliquot of freeze-dried sediment (between 50 and 150 mg) was incubated in 10 mL of a solution of ascorbic acid (buffered at pH 8) during 24 hours to extract the reactive solid phase. This technique is commonly used (Anschutz et al., 1998; Hyacinthe et al., 2001; Hyacinthe and Van Cappellen, 2004; Kostka and Luther III, 1995) and allows to extract both amorphous Fe(III) oxyhydroxides (Kostka and Luther III, 1994) supposedly close to those reduced by microorganisms (Hyacinthe et al., 2006) as well as Mn(III) and Mn(IV) oxides (Anschutz et al., 2005). After extraction, samples were centrifuged (15 mn at 3000 rpm) and the supernatant was diluted in Ultrapure© HCl (1% weight). Next, samples were analyzed on ICP-AES (Thermo Scientific iCAP 6300 Radial), incertitude is 1, 8 and 4% for respectively iron, phosphorus and manganese (twice the relative standard deviation of ICP-AES triplicates). The second aliquot, between 1.5 and 3 mg, was used for organic carbon analysis. It was performed on EA1110 CHN/S/O (Thermo Fisher) after 1h-extraction in a HCl saturated atmosphere. Each chromatograph was inspected visually. Accuracy was verified with standards (MS-61 and B2150) and incertitude, calculated from standard deviation for ten replicates from standard MS-61, was 4.5%.

S2 1D Pore water analysis

Oxygen, dissolved iron, manganese and phosphorus were analyzed. The core dedicated to oxygen profiling and solid phase remained emerged in the *in situ* temperature tank. The

sediment water interface was roughly visually estimated during profiling. During data treatment, the interface was repositioned according to the break visible in the O_2 profile after the start of the concentration decrease. 18 oxygen profiles (each time two profiles were measured simultaneously) were realized using Clark's type electrodes (50µm tip diameter) mounted on an automated micromanipulator (Unisense©, Denmark) within the first 5 mm at a 100 µm vertical resolution. Profiling was done within 1 hour after sampling.

Diffusive Equilibrium in Thin film in one dimension probes (DET 1D, adapted from Davison and Zhang, 1994; Krom et al., 1994) were used for dissolved iron, manganese and phosphorus. Two probes were prepared from DGT-Research© supports, less than one week before deployment. Each support corresponds to 75 cells of 22 µL and has a vertical resolution of 2 mm. They were cleaned during 1 week using 10 % Suprapur Merck nitric acid and rinsed three time with milli-Q water (Millipore©). A solution (1.5% w/w) of agarose in Milli-Q water was poured into the probe, the excess gel was removed with a Teflon-coated razor blade and then covered with a PVDF hydrophilic membrane (0.2 µm size pore, Millipore©) (Metzger et al., 2007, 2014). Each probe was conserved in a wet clean plastic bag and finally bubbled with N_2 during 6h before deployment in the third core. After one night incubation in the core at *in situ* temperature, probes were retrieved and DET gel pieces were sampled using a small plastic tip and eluted in 5mL of a 0.01 mol L^{-1} suprapur© Merck nitric acid solution (dilution factor of the pore water of about 200). Iron, manganese and phosphorus were then analyzed by ICP-AES (Thermo Scientific iCAP 6300 Radial). Sodium was supposed constant through the sediment column, and used as internal standard. Incertitude is less than 10% for dissolved iron and manganese and 30% for phosphorus.

S3 2D pore water analysis

The DET 2D probe was analyzed in order to obtain the concentrations of dissolved iron, dissolved reactive phosphate (DRP) and the qualitative distribution of H_2S (Cesbron et al., 2014). The 2D DET probe was unfrozen during 10 minutes at ambient temperature; next, the plastic-coated aluminum plate was taken out and the polyacrylamide thin-film was taken off. The PVC adhesive film was scanned with a common commercial flatbed scanner (Canon Canoscan LiDE 600F) and analyzed in blue intensity (from RGB decomposition) with ImageJ© software. The unfrozen gel is laid on a white board and recovered by a reactive gel.

699 The reactive gel was a 0.46mm thick polyacrylamide gel incubated during 1 hour in a reactive
700 solution containing ascorbic acid 3 10^{-2}M, sulfuric acid 5.58 10^{-1}M, potassium antimony(III)
701 tartrate hydrate 3.2 10^{-4}M, ammonium molybdate tetrahydrate 1.86 10^{-2}M and ferrozine 1.22
702 10^{-2}M, final concentrations. This is an improvement compared to Cesbron et al. (2014) as
703 only one reactive gel is made, instead of two, reducing handling time considerably.
704
705 Twenty five minutes after contact, a picture (reflectance analysis) of superposed gels was
706 taken with a hyperspectral camera (HySpex VNIR 1600) and analyzed with the software
707 ENVI (Environment for Visualizing Image, RSI) to obtain DRP and dissolved iron
708 concentrations. The resolution (length of pixels) was 211*216µm^2. The HySpex VNIR 1600
709 camera is sensitive to 160 channels (spectral resolution of 4.5 nm), which is much more
710 precise than the three channels of 100 nm resolution from standard RGB (Red, Green, Blue)
711 images. Standards, made following (Cesbron et al., 2014) gave one end-member spectrum for
712 each measured species (mean of 2470±5 pixels) and a third end-member spectrum for the
713 background (Fig 4). Next, after logarithmic transformation of reflectance, linear combination
714 between these three end-members applied on each pixel (of both standard and probe gels),
715 gave the proportion of each one expressed on that pixel. For the two chemical species, this
716 proportion was multiplied by the respective known concentration of end-members (here 18.58
717 µM for DRP and 253.56 µM for dissolved iron). Next, a calibration with the standard is made
718 (six points for each species: from 3.52 to 59.31 µM for DRP and from 16.46 to 253.56 µM for
719 iron). The exactness of the method is verified by 1) comparison between measured+calculated
720 and real concentrations of standards (mean difference of 4,4% for iron and 7,3% for DRP), 2)
721 the expression of background end-members from linear combination (here 0.95±0.06
722 compared to the theoretical value of 1.00) and 3) the error from linear combination, here of
723 3.4±0.5%. The estimated complete incertitude is then 9,8% for iron and 11,2% for DRP.
724
725 To compare the geochemical species distribution (at submillimeter resolution) with
726 foraminiferal density (at centimeter resolution), a handmade R code was written allowing the
727 decrease of chemical resolution from 0.2 mm down to 1 cm. As 1 centimeter is equal to
728 46.3*47.4 pixels, the code takes for each centimeter the average concentration of 46*47=2162
729 pixels. Thus 0.3*0.4 pixels are lost for each centimeter square which correspond to 1.27% of
730 the surface *i.e.* 2.3 cm^2 for the entire gel. This loss is attributed to each side, and then
731 neglected.
732

Acknowledgements

This study is part of the RS2E – OSUNA project funded by the Région Pays de la Loire. Special thanks are due to Didier Jézéquel from IPGP who designed the « jaw device". Thanks to Clement Chauvin, Cyrille Guindir, Hélène Koroshidi and Eve Chauveau for their support in the field and laboratory. We thank the three editorial reviewers whose comments inspired us to improve our manuscript.

References

Aller, J. Y. and Aller, R. C.: Evidence for localized enhancement of biological associated with tube and burrow structures in deep-sea sediments at the HEEBLE site, western North Atlantic, Deep Sea Res. Part Oceanogr. Res. Pap., 33(6), 755–790, doi:10.1016/0198-0149(86)90088-9, 1986.

Aller, R. C.: The Effects of Macrobenthos on Chemical Properties of Marine Sediment and Overlying Water, in Animal-Sediment Relations, edited by P. L. McCall and M. J. S. Tevesz, pp. 53–102, Springer US. [online] Available from: http://link.springer.com/chapter/10.1007/978-1-4757-1317-6_2 (Accessed 22 August 2014), 1982.

Aller, R. C.: Conceptual models of early diagenetic processes: The muddy seafloor as an unsteady, batch reactor, J. Mar. Res., 62(6), 815–835, doi:10.1357/0022240042880837, 2004.

Alve, E. and Bernhard, J. M.: Vertical migratory response of benthic foraminifera to controlled oxygen concentrations in an experimental mesocosm, Oceanogr. Lit. Rev., 42(9), 137–151, doi:http://dx.doi.org/10.3354/meps116137, 1995.

Alve, E. and Murray, J. W.: Temporal Variability in Vertical Distributions of Live (stained) Intertidal Foraminifera, Southern England, J. Foraminifer. Res., 31(1), 12–24, doi:10.2113/0310012, 2001.

Anschutz, P., Dedieu, K., Desmazes, F. and Chaillou, G.: Speciation, oxidation state, and reactivity of particulate manganese in marine sediments, Chem. Geol., 218(3–4), 265–279, doi:10.1016/j.chemgeo.2005.01.008, 2005.

Anschutz, P., Zhong, S., Sundby, B., Mucci, A. and Gobeil, C.: Burial efficiency of phosphorus and the geochemistry of iron in continental margin sediments, Limnol. Oceanogr., 43(1), 53–64, 1998.

Arndt, S., Jørgensen, B. B., LaRowe, D. E., Middelburg, J. J., Pancost, R. D. and Regnier, P.: Quantifying the degradation of organic matter in marine sediments: A review and synthesis, Earth-Sci. Rev., 123, 53–86, doi:10.1016/j.earscirev.2013.02.008, 2013.

Barmawidjaja, D. M., Jorissen, F. J., Puskaric, S. and Zwaan, G. J. van der: Microhabitat selection by benthic Foraminifera in the northern Adriatic Sea, J. Foraminifer. Res., 22(4), 297–317, doi:10.2113/gsjfr.22.4.297, 1992.

Bennett, W. W., Welsh, D. T., Serriere, A., Panther, J. G. and Teasdale, P. R.: A colorimetric DET technique for the high-resolution measurement of two-dimensional alkalinity distributions in sediment porewaters, Chemosphere, 119, 547–552, doi:10.1016/j.chemosphere.2014.07.042, 2015.

Benyoucef, I.: Télédétection visible proche-infrarouge de la distribution spatio-temporelle du microphytobenthos estuarien, Ph.D. thesis, Université de Nantes, 4 August., 2014.

Benyoucef, I., Blandin, E., Lerouxel, A., Jesus, B., Rosa, P., Méléder, V., Launeau, P. and Barillé, L.: Microphytobenthos interannual variations in a north-European estuary (Loire estuary, France) detected by visible-infrared multispectral remote sensing, Estuar. Coast. Shelf Sci., 136, 43–52, doi:10.1016/j.ecss.2013.11.007, 2014.

Berg, P., Risgaard-Petersen, N. and Rysgaard, S.: Interpretation of measured concentration profiles in sediment pore water, Limnol. Oceanogr., 43(7), 1500–1510, doi:10.4319/lo.1998.43.7.1500, 1998.

Berkeley, A., Perry, C. T., Smithers, S. G., Horton, B. P. and Taylor, K. G.: A review of the ecological and taphonomic controls on foraminiferal assemblage development in intertidal environments, Earth-Sci. Rev., 83(3-4), 205–230, doi:10.1016/j.earscirev.2007.04.003, 2007.

Berner, R. A.: Sedimentary pyrite formation, Am. J. Sci., 268(1), 1–23, doi:10.2475/ajs.268.1.1, 1970.

Bernhard, J. M. and Alve, E.: Survival, ATP pool, and ultrastructural characterization of benthic foraminifera from Drammensfjord (Norway): response to anoxia, Mar. Micropaleontol., 28(1), 5–17, doi:10.1016/0377-8398(95)00036-4, 1996.

Bernhard, J. M., Ostermann, D. R., Williams, D. S. and Blanks, J. K.: Comparison of two methods to identify live benthic foraminifera: A test between Rose Bengal and CellTracker Green with implications for stable isotope paleoreconstructions, Paleoceanography, 21(4), PA4210, doi:10.1029/2006PA001290, 2006.

Bernhard, J. M. and Sen Gupta, B. K. S.: Foraminifera of oxygen-depleted environments, in Modern Foraminifera, pp. 201–216, Springer Netherlands. [online] Available from: http://link.springer.com/chapter/10.1007/0-306-48104-9_12 (Accessed 27 November 2014), 2003.

Bivand, R., Pebesma, E. and Gomez-Rubio, V.: Applied Spatial Data Analysis with R, Springer New York, New York, NY. [online] Available from: http://link.springer.com/10.1007/978-0-387-78171-6 (Accessed 16 August 2014), 2008.

Blanchard, G.: Overlapping microscale dispersion patterns of meiofauna and microphytobenthos, Mar. Ecol. Prog. Ser., 68, 101–111, doi:10.3354/meps068101, 1990.

Borcard, D., Gillet, F. and Legendre, P.: Numerical Ecology with R, Springer New York, New York, NY. [online] Available from: http://link.springer.com/10.1007/978-1-4419-7976-6 (Accessed 16 August 2014), 2011.

Bouchet, V. M. P., Sauriau, P.-G., Debenay, J.-P., Mermillod-Blondin, F., Schmidt, S., Amiard, J.-C. and Dupas, B.: Influence of the mode of macrofauna-mediated bioturbation on the vertical distribution of living benthic foraminifera: First insight from axial

tomodensitometry, J. Exp. Mar. Biol. Ecol., 371(1), 20–33, doi:10.1016/j.jembe.2008.12.012, 2009.

Boudreau, B. P.: A method-of-lines code for carbon and nutrient diagenesis in aquatic sediments, Comput. Geosci., 22(5), 479–496, 1996.

Burdige, D. J.: 5.09 - Estuarine and Coastal Sediments – Coupled Biogeochemical Cycling, in Treatise on Estuarine and Coastal Science, edited by E. Wolanski and D. McLusky, pp. 279–316, Academic Press, Waltham. [online] Available from: http://www.sciencedirect.com/science/article/pii/B9780123747112005118 (Accessed 26 March 2015), 2011.

Buzas: On the spatial distribution of foraminifera:, Contrib. Cushman Found. Foraminifer. Res., 19, 1–11, 1968.

Buzas, M. A.: Spatial Homogeneity: Statistical Analyses of Unispecies and Multispecies Populations of Foraminifera, Ecology, 51(5), 874, doi:10.2307/1933980, 1970.

Buzas, M. A., Hayek, L.-A. C., Jett, J. A. and Reed, S. A.: Pulsating Patches: History and Analyses of Spatial, Seasonal, and Yearly Distribution of Living Benthic Foraminifera, Smithson. Contrib. Paleobiology, (97), 2015.

Buzas, M. A., Hayek, L.-A. C., Reed, S. A. and Jett, J. A.: Foraminiferal Densities Over Five Years in the Indian River Lagoon, Florida: A Model of Pulsating Patches, J. Foraminifer. Res., 32(1), 68–92, doi:10.2113/0320068, 2002.

Cesbron, F., Metzger, E., Launeau, P., Deflandre, B., Delgard, M.-L., Thibault de Chanvalon, A., Geslin, E., Anschutz, P. and Jézéquel, D.: Simultaneous 2D Imaging of Dissolved Iron and Reactive Phosphorus in Sediment Porewaters by Thin-Film and Hyperspectral Methods, Environ. Sci. Technol., 48(5), 2816–2826, doi:10.1021/es404724r, 2014.

Clark, W. C.: Scales of climate impacts, Clim. Change, 7(1), 5–27, 1985.

Davison, W. and Zhang, H.: In situspeciation measurements of trace components in natural waters using thin-film gels, Nature, 367(6463), 546–548, doi:10.1038/367546a0, 1994.

Debenay, J.-P., Bicchi, E., Goubert, E. and Armynot du Châtelet, E.: Spatio-temporal distribution of benthic foraminifera in relation to estuarine dynamics (Vie estuary, Vendée, W France), Estuar. Coast. Shelf Sci., 67(1–2), 181–197, doi:10.1016/j.ecss.2005.11.014, 2006.

Debenay, J.-P. and Guillou, J.-J.: Ecological transitions indicated by foraminiferal assemblages in paralic environments, Estuaries, 25(6), 1107–1120, doi:10.1007/BF02692208, 2002.

Douglas, R. G.: Paleoecology of continental margin basins: a modern case history from the borderland of southern California, 1981.

Eckman, J. E. and Thistle, D.: Small-scale spatial pattern in meiobenthos in the San Diego Trough, Deep Sea Res. Part Oceanogr. Res. Pap., 35(9), 1565–1578, doi:10.1016/0198-0149(88)90103-3, 1988.

847 Ernst, S., Bours, R., Duijnstee, I. and van der Zwaan, B.: Experimental effects of an organic
848 matter pulse and oxygen depletion on a benthic foraminiferal shelf community, J.
849 Foraminifer. Res., 35(3), 177–197, 2005.

850 Ernst, S. R., Morvan, J., Geslin, E., Le Bihan, A. and Jorissen, F. J.: Benthic foraminiferal
851 response to experimentally induced Erika oil pollution, Mar. Micropaleontol., 61(1-3), 76–93,
852 doi:10.1016/j.marmicro.2006.05.005, 2006.

853 Fenchel, T.: Worm burrows and oxic microniches in marine sediments. 1. Spatial and
854 temporal scales, Mar. Biol., 127(2), 289–295, doi:10.1007/BF00942114, 1996.

855 Fontanier, C., Jorissen, F. J., Licari, L., Alexandre, A., Anschutz, P. and Carbonel, P.: Live
856 benthic foraminiferal faunas from the Bay of Biscay: faunal density, composition, and
857 microhabitats, Deep Sea Res. Part Oceanogr. Res. Pap., 49(4), 751–785, doi:10.1016/S0967-
858 0637(01)00078-4, 2002.

859 Fortin, M.-J. and Dale, M. R. T.: Spatial analysis a guide for ecologists, Cambridge
860 University Press, Cambridge, N.Y. [online] Available from:
861 http://public.eblib.com/EBLPublic/PublicView.do?ptiID=228304 (Accessed 16 August 2014),
862 2005.

863 François, F., Gerino, M., Stora, G., Durbec, J. and Poggiale, J.: Functional approach to
864 sediment reworking by gallery-forming macrobenthic organisms: modeling and application
865 with the polychaete Nereis diversicolor, Mar. Ecol. Prog. Ser., 229, 127–136,
866 doi:10.3354/meps229127, 2002.

867 Froelich, P. N., Klinkhammer, G. P., Bender, M. L., Luedtke, N. A., Heath, G. R., Cullen, D.,
868 Dauphin, P., Hammond, D., Hartman, B. and Maynard, V.: Early oxidation of organic matter
869 in pelagic sediments of the eastern equatorial Atlantic: suboxic diagenesis, Geochim.
870 Cosmochim. Acta, 43(7), 1075–1090, doi:10.1016/0016-7037(79)90095-4, 1979.

871 Geslin, E., Barras, C., Langlet, D., Nardelli, M. P., Kim, J.-H., Bonnin, J., Metzger, E. and
872 Jorissen, F. J.: Survival, Reproduction and Calcification of Three Benthic Foraminiferal
873 Species in Response to Experimentally Induced Hypoxia, in Approaches to Study Living
874 Foraminifera, edited by H. Kitazato and J. M. Bernhard, pp. 163–193, Springer Japan.
875 [online] Available from: http://link.springer.com/chapter/10.1007/978-4-431-54388-6_10
876 (Accessed 20 August 2014), 2014.

877 Geslin, E., Heinz, P., Jorissen, F. and Hemleben, C.: Migratory responses of deep-sea benthic
878 foraminifera to variable oxygen conditions: laboratory investigations, Mar. Micropaleontol.,
879 53(3–4), 227–243, doi:10.1016/j.marmicro.2004.05.010, 2004.

880 Goldstein, S. T., Watkins, G. T. and Kuhn, R. M.: Microhabitats of salt marsh foraminifera:
881 St. Catherines Island, Georgia, USA, Mar. Micropaleontol., 26(1–4), 17–29,
882 doi:10.1016/0377-8398(95)00006-2, 1995.

883 Gross, O.: Influence of temperature, oxygen and food availability on the migrational activity
884 of bathyal benthic foraminifera: evidence by microcosm experiments, in Life at Interfaces and
885 Under Extreme Conditions, edited by G. Liebezeit, S. Dittmann, and I. Kröncke, pp. 123–137,
886 Springer Netherlands. [online] Available from: http://link.springer.com/chapter/10.1007/978-
887 94-011-4148-2_12 (Accessed 3 October 2014), 2000.

Heinz, P. and Geslin, E.: Ecological and Biological Response of Benthic Foraminifera Under Oxygen-Depleted Conditions: Evidence from Laboratory Approaches, in Anoxia, edited by A. V. Altenbach, J. M. Bernhard, and J. Seckbach, pp. 287–303, Springer Netherlands. [online] Available from: http://link.springer.com/chapter/10.1007/978-94-007-1896-8_15 (Accessed 7 January 2015), 2012.

Hess, S., Alve, E., Trannum, H. C. and Norling, K.: Benthic foraminiferal responses to water-based drill cuttings and natural sediment burial: Results from a mesocosm experiment, Mar. Micropaleontol., 101, 1–9, doi:10.1016/j.marmicro.2013.03.004, 2013.

Hofmann, A. F., Soetaert, K., Middelburg, J. J. and Meysman, F. J. R.: AquaEnv : An Aqua tic Acid–Base Modelling Env ironment in R, Aquat. Geochem., 16(4), 507–546, doi:10.1007/s10498-009-9084-1, 2010.

Hohenegger, J., Piller, W. and Baal, C.: Reasons for spatial microdistributions of foraminifers in an intertidal pool (northern Adriatic Sea), Mar. Ecol., 10(1), 43–78, 1989.

Hohenegger, J., Piller, W. E. and Baal, C.: Horizontal and vertical spatial microdistribution of foraminifers in the shallow subtidal Gulf of Trieste, northern Adriatic Sea, J. Foraminifer. Res., 23(2), 79–101, doi:10.2113/gsjfr.23.2.79, 1993.

Hyacinthe, C., Anschutz, P., Carbonel, P., Jouanneau, J.-M. and Jorissen, F. J.: Early diagenetic processes in the muddy sediments of the Bay of Biscay, Mar. Geol., 177(1–2), 111–128, doi:10.1016/S0025-3227(01)00127-X, 2001.

Hyacinthe, C., Bonneville, S. and Van Cappellen, P.: Reactive iron(III) in sediments: Chemical versus microbial extractions, Geochim. Cosmochim. Acta, 70(16), 4166–4180, doi:10.1016/j.gca.2006.05.018, 2006.

Hyacinthe, C. and Van Cappellen, P.: An authigenic iron phosphate phase in estuarine sediments: composition, formation and chemical reactivity, Mar. Chem., 91(1-4), 227–251, doi:10.1016/j.marchem.2004.04.006, 2004.

Jézéquel, D., Brayner, R., Metzger, E., Viollier, E., Prévot, F. and Fiévet, F.: Two-dimensional determination of dissolved iron and sulphur species in marine sediment pore-waters by thin-film based imaging. Thau lagoon (France), Estuar. Coast. Shelf Sci., 72(3), 420–431, doi:10.1016/j.ecss.2006.11.031, 2007.

Jorissen, F. J.: Benthic foraminifera from the Adriatic Sea: principles of phenotypic variation, Utrecht Micropaleontol. Bull., 37, 1988.

Jorissen, F. J.: Benthic foraminiferal microhabitats below the sediment-water interface, in Modern Foraminifera, pp. 161–179, Springer Netherlands. [online] Available from: http://link.springer.com/chapter/10.1007/0-306-48104-9_10 (Accessed 20 August 2014), 2003.

Jorissen, F. J., Barmawidjaja, D. M., Puskaric, S. and van der Zwaan, G. J.: Vertical distribution of benthic foraminifera in the northern Adriatic Sea: The relation with the organic flux, Mar. Micropaleontol., 19(1–2), 131–146, doi:10.1016/0377-8398(92)90025-F, 1992.

Jorissen, F. J., de Stigter, H. C. and Widmark, J. G. V.: A conceptual model explaining benthic foraminiferal microhabitats, Mar. Micropaleontol., 26(1–4), 3–15, doi:10.1016/0377-8398(95)00047-X, 1995.

Jorissen, F. J., Wittling, I., Peypouquet, J. P., Rabouille, C. and Relexans, J. C.: Live benthic foraminiferal faunas off Cape Blanc, NW-Africa: Community structure and microhabitats, Deep Sea Res. Part Oceanogr. Res. Pap., 45(12), 2157–2188, doi:10.1016/S0967-0637(98)00056-9, 1998.

Koller, H., Dworschak, P. C. and Abed-Navandi, D.: Burrows of Pestarella tyrrhena (Decapoda: Thalassinidea): hot spots for Nematoda, Foraminifera and bacterial densities, J. Mar. Biol. Assoc. U. K., 86(5), 1113–1122, 2006.

Kostka, J. E. and Luther III, G. W.: Seasonal cycling of Fe in saltmarsh sediments, Biogeochemistry, 29(2), 159–181, 1995.

Kristensen, E., PenhaLopes, G., Delefosse, M., Valdemarsen, T., Quintana, C. O. and Banta, G. T.: REVIEW What is bioturbation? The need for a precise definition for fauna in aquatic sciences, Mar. Ecol. Prog. Ser., 446, 285–302, doi:10.3354/meps09506, 2012.

Krom, M. D., Davison, P., Zhang, H. and Davison, W.: High-resolution pore-water sampling with a gel sampler, Limnol. Oceanogr., 39(8), 1967–1972, 1994.

Langezaal, A. M., Ernst, S. R., Haese, R. R., van Bergen, P. F. and van der Zwaan, G. J.: Disturbance of intertidal sediments: the response of bacteria and foraminifera, Estuar. Coast. Shelf Sci., 58(2), 249–264, doi:10.1016/S0272-7714(03)00078-7, 2003.

Langezaal, A. M., Jorissen, F. J., Braun, B., Chaillou, G., Fontanier, C., Anschutz, P. and van der Zwaan, G. J.: The influence of seasonal processes on geochemical profiles and foraminiferal assemblages on the outer shelf of the Bay of Biscay, Cont. Shelf Res., 26(15), 1730–1755, doi:10.1016/j.csr.2006.05.005, 2006.

Langlet, D., Geslin, E., Baal, C., Metzger, E., Lejzerowicz, F., Riedel, B., Zuschin, M., Pawlowski, J., Stachowitsch, M. and Jorissen, F. J.: Foraminiferal survival after long-term in situ experimentally induced anoxia, Biogeosciences, 10(11), 7463–7480, doi:10.5194/bg-10-7463-2013, 2013.

Le Floch, J.-F.: Propagation de la marée dynamique dans l'estuaire de la Seine et en Seine maritime., Thèse d'Etat, Paris., 1961.

Legendre and Fortin: Spatial pattern and ecological analysis, Vegetation, 80, 107–138, 1989.

Legendre, P. and Fortin, M.-J.: Comparison of the Mantel test and alternative approaches for detecting complex multivariate relationships in the spatial analysis of genetic data, Mol. Ecol. Resour., 10(5), 831–844, doi:10.1111/j.1755-0998.2010.02866.x, 2010.

Leutenegger, S. and Hansen, H. J.: Ultrastructural and radiotracer studies of pore function in foraminifera, Mar. Biol., 54(1), 11–16, doi:10.1007/BF00387046, 1979.

Loubere, P., Jacobsen, B., Klitgaard Kristensen, D., Husum, K., Jernas, P. and Richaud, M.: The structure of benthic environments and the paleochemical record of foraminifera, Deep Sea Res. Part Oceanogr. Res. Pap., 58(5), 535–545, doi:10.1016/j.dsr.2011.02.011, 2011.

965 Lovley, D. R.: Dissimilatory Fe(III) and Mn(IV) reduction., Microbiol. Rev., 55(2), 259–287,
966 1991.

967 Lynts, G. W.: Relationship of Sediment-size Distribution to Ecologic Factors in Buttonwood
968 Sound, Florida Bay, J. Sediment. Res., 36(1) [online] Available from:
969 http://archives.datapages.com/data/sepm/journals/v33-37/data/036/036001/0066.htm
970 (Accessed 27 November 2014), 1966.

971 Martiny, J. B. H., Bohannan, B. J. M., Brown, J. H., Colwell, R. K., Fuhrman, J. A., Green, J.
972 L., Horner-Devine, M. C., Kane, M., Krumins, J. A., Kuske, C. R., Morin, P. J., Naeem, S.,
973 Øvreås, L., Reysenbach, A.-L., Smith, V. H. and Staley, J. T.: Microbial biogeography:
974 putting microorganisms on the map, Nat. Rev. Microbiol., 4(2), 102–112,
975 doi:10.1038/nrmicro1341, 2006.

976 Meyers, M. B., Fossing, H. and Powell, E. N.: Microdistribution of interstitial meiofauna,
977 oxygen and sulphide gradients, and the tubes of macro-infauna, Mar. Ecol.-Prog. Ser., 35,
978 223–241, doi:10.3354/meps035223, 1987.

979 Meysman, F. J., Boudreau, B. P. and Middelburg, J. J.: When and why does bioturbation lead
980 to diffusive mixing?, J. Mar. Res., 68(6), 881–920, 2010a.

981 Meysman, F. J. R., Boudreau, B. P. and Middelburg, J. J.: Relations between local, nonlocal,
982 discrete and continuous models of bioturbation, J. Mar. Res., 61(3), 391–410,
983 doi:10.1357/002224003322201241, 2003.

984 Meysman, F. J. R., Galaktionov, O. S., Glud, R. N. and Middelburg, J. J.: Oxygen penetration
985 around burrows and roots in aquatic sediments, J. Mar. Res., 68(2), 309–336,
986 doi:10.1357/002224010793721406, 2010b.

987 Meysman, F. J. R., Malyuga, V. S., Boudreau, B. P. and Middelburg, J. J.: A generalized
988 stochastic approach to particle dispersal in soils and sediments, Geochim. Cosmochim. Acta,
989 72(14), 3460–3478, doi:10.1016/j.gca.2008.04.023, 2008.

990 Meysman, F. J. R., Middelburg, J. J. and Heip, C. H. R.: Bioturbation: a fresh look at
991 Darwin's last idea, Trends Ecol. Evol., 21(12), 688–695, doi:10.1016/j.tree.2006.08.002,
992 2006.

993 Millero, F. J.: The thermodynamics of the carbonate system in seawater, Geochim.
994 Cosmochim. Acta, 43(10), 1651–1661, doi:10.1016/0016-7037(79)90184-4, 1979.

995 Millero, F. J.: Thermodynamics of the carbon dioxide system in the oceans, Geochim.
996 Cosmochim. Acta, 59(4), 661–677, doi:10.1016/0016-7037(94)00354-O, 1995.

997 Moodley, L.: Southern North Sea seafloor and subsurface distribution of living benthic
998 foraminifera, Neth. J. Sea Res., 27(1), 57–71, doi:10.1016/0077-7579(90)90034-E, 1990.

999 Moodley, L. and Hess, C.: Tolerance of Infaunal Benthic Foraminifera for Low and High
1000 Oxygen Concentrations, Biol. Bull., 183(1), 94–98, 1992.

1001 Moodley, L., van der Zwaan, G. J., Rutten, G. M. W., Boom, R. C. E. and Kempers, A. J.:
1002 Subsurface activity of benthic foraminifera in relation to porewater oxygen content:

laboratory experiments, Mar. Micropaleontol., 34(1–2), 91–106, doi:10.1016/S0377-8398(97)00044-3, 1998.

Morse, J. W., DiMarco, S. F., Hebert, A. B. and Sell, K. S.: A scaling approach to spatial variability in early diagenetic processes, in The Interactions between Sediments and Water, pp. 25–29, Springer. [online] Available from: http://link.springer.com/chapter/10.1007/978-94-017-3366-3_5 (Accessed 30 June 2014), 2003.

Morvan, J., Debenay, J.-P., Jorissen, F., Redois, F., Bénéteau, E., Delplancke, M. and Amato, A.-S.: Patchiness and life cycle of intertidal foraminifera: Implication for environmental and paleoenvironmental interpretation, Mar. Micropaleontol., 61(1-3), 131–154, doi:10.1016/j.marmicro.2006.05.009, 2006.

Mucci, A.: The solubility of calcite and aragonite in seawater at various salinities, temperatures, and one atmosphere total pressure, Am. J. Sci., 283(7), 780–799, doi:10.2475/ajs.283.7.780, 1983.

Mucci, A., Sundby, B., Gehlen, M., Arakaki, T., Zhong, S. and Silverberg, N.: The fate of carbon in continental shelf sediments of eastern Canada: a case study, Deep Sea Res. Part II Top. Stud. Oceanogr., 47(3–4), 733–760, doi:10.1016/S0967-0645(99)00124-1, 2000.

Nardelli, M. P., Barras, C., Metzger, E., Mouret, A., Filipsson, H. L., Jorissen, F. and Geslin, E.: Experimental evidence for foraminiferal calcification under anoxia, Biogeosciences, 11(14), 4029–4038, doi:10.5194/bg-11-4029-2014, 2014.

Nomaki, H., Chikaraishi, Y., Tsuchiya, M., Toyofuku, T., Ohkouchi, N., Uematsu, K., Tame, A. and Kitazato, H.: Nitrate uptake by foraminifera and use in conjunction with endobionts under anoxic conditions, Limnol. Oceanogr., 59(6), 1879–1888, doi:10.4319/lo.2014.59.6.1879, 2014.

Paterson, D. M.: Short-term changes in the erodibility of intertidal cohesive sediments related to the migratory behavior of epipelic diatoms, Limnol. Oceanogr., 34(1), 223–234, 1989.

Phipps, M. Daniel: Benthic foraminifera of the Portuguese margin: Impact of organic supplies on the density, biodiversity and composition of the faunas, Université d'Angers. [online] Available from: https://tel.archives-ouvertes.fr/tel-00993121/ (Accessed 28 April 2015), 2012.

Pina-Ochoa, E., Hogslund, S., Geslin, E., Cedhagen, T., Revsbech, N. P., Nielsen, L. P., Schweizer, M., Jorissen, F., Rysgaard, S. and Risgaard-Petersen, N.: Widespread occurrence of nitrate storage and denitrification among Foraminifera and Gromiida, Proc. Natl. Acad. Sci., 107(3), 1148–1153, doi:10.1073/pnas.0908440107, 2010.

Pischedda, L., Cuny, P., Esteves, J. L., Poggiale, J.-C. and Gilbert, F.: Spatial oxygen heterogeneity in a Hediste diversicolor irrigated burrow, Hydrobiologia, 680(1), 109–124, doi:10.1007/s10750-011-0907-x, 2012.

Pucci, F., Geslin, E., Barras, C., Morigi, C., Sabbatini, A., Negri, A. and Jorissen, F. J.: Survival of benthic foraminifera under hypoxic conditions: Results of an experimental study using the CellTracker Green method, Mar. Pollut. Bull., 59(8–12), 336–351, doi:10.1016/j.marpolbul.2009.08.015, 2009.

1042 Revsbech, N. P., SøRensen, J., Blackburn, T. H. and Lomholt, J. P.: Distribution of oxygen in
1043 marine sediments measured with microelectrodes, Limnol. Oceanogr., 25(3), 403–411,
1044 doi:10.4319/lo.1980.25.3.0403, 1980.

1045 Richter, G.: Beobachtungen zur O¨ kologie einiger Foraminiferen des Jade Gebietes, Nat.
1046 Volk, 91, 163–170, 1961.

1047 Risgaard-Petersen, N., Langezaal, A. M., Ingvardsen, S., Schmid, M. C., Jetten, M. S. M., Op
1048 den Camp, H. J. M., Derksen, J. W. M., Piña-Ochoa, E., Eriksson, S. P., Peter Nielsen, L.,
1049 Peter Revsbech, N., Cedhagen, T. and van der Zwaan, G. J.: Evidence for complete
1050 denitrification in a benthic foraminifer, Nature, 443(7107), 93–96, doi:10.1038/nature05070,
1051 2006.

1052 Robertson, D., Teasdale, P. R. and Welsh, D. T.: A novel gel-based technique for the high
1053 resolution, two-dimensional determination of iron (II) and sulphide in sediment, Limnol
1054 Ocean. Methods, 6, 502–512, 2008.

1055 Robertson, D., Welsh, D. T. and Teasdale, P. R.: Investigating biogenic heterogeneity in
1056 coastal sediments with two-dimensional measurements of iron(II) and sulphide, Environ.
1057 Chem., 6(1), 60–69, 2009.

1058 Round, F.: The ecology of benthic algae, in Algae and man, pp. 138–184, Springer., 1964.

1059 Saffert, H. and Thomas, E.: Living foraminifera and total populations in salt marsh peat cores:
1060 Kelsey Marsh (Clinton, CT) and the Great Marshes (Barnstable, MA), Mar. Micropaleontol.,
1061 33(3–4), 175–202, doi:10.1016/S0377-8398(97)00035-2, 1998.

1062 Santner, J., Larsen, M., Kreuzeder, A. and Glud, R. N.: Two decades of chemical imaging of
1063 solutes in sediments and soils – a review, Anal. Chim. Acta, doi:10.1016/j.aca.2015.02.006,
1064 2015.

1065 de Stigter, H. C., van der Zwaan, G. J. and Langone, L.: Differential rates of benthic
1066 foraminiferal test production in surface and subsurface sediment habitats in the southern
1067 Adriatic Sea, Palaeogeogr. Palaeoclimatol. Palaeoecol., 149(1–4), 67–88, doi:10.1016/S0031-
1068 0182(98)00193-X, 1999.

1069 Stockdale, A., Davison, W. and Zhang, H.: Micro-scale biogeochemical heterogeneity in
1070 sediments: A review of available technology and observed evidence, Earth-Sci. Rev., 92(1–2),
1071 81–97, doi:10.1016/j.earscirev.2008.11.003, 2009.

1072 Stockdale, A., Davison, W. and Zhang, H.: Formation of iron sulphide at faecal pellets and
1073 other microniches within suboxic surface sediment, Geochim. Cosmochim. Acta, 74(9),
1074 2665–2676, doi:10.1016/j.gca.2010.02.005, 2010.

1075 Thibault de Chanvalon, A., Metzger, E., Mouret, A., Geslin, E., Knoery, J. and Meysman, F.
1076 J. R.: Iron release from intertidal mudflat: 2D modelling at submillimetre scale., Mar. Chem.,
1077 in prep.

1078 Thomsen, L. and Altenbach, A. V.: Vertical and areal distribution of foraminiferal abundance
1079 and biomass in microhabitats around inhabited tubes of marine echiurids, Mar.
1080 Micropaleontol., 20(3–4), 303–309, doi:10.1016/0377-8398(93)90039-Z, 1993.

Travis, J. L. and Rabalais, N. N.: The motility of Foraminifera, in Biology of the Foraminifera, in Biology of the Foraminifera, pp. 91–155, J.J. Lee O.R. Anderson, London., 1991.

Vader, W. J. M.: A preliminary investigation into the reactions of the infauna of the tidal flats to tidal fluctuations in water level, Neth. J. Sea Res., 2(2), 189–222, doi:10.1016/0077-7579(64)90009-2, 1964.

Van der Zwaan, G. J., Duijnstee, I. A. P., den Dulk, M., Ernst, S. R., Jannink, N. T. and Kouwenhoven, T. J.: Benthic foraminifers: proxies or problems?: A review of paleocological concepts, Earth-Sci. Rev., 46(1–4), 213–236, doi:10.1016/S0012-8252(99)00011-2, 1999.

Van der Zwaan, G. J. V. D. and Jorissen, F. J.: Biofacial patterns in river-induced shelf anoxia, Geol. Soc. Lond. Spec. Publ., 58(1), 65–82, doi:10.1144/GSL.SP.1991.058.01.05, 1991.

Wang, F., Tessier, A. and Hare, L.: Oxygen measurements in the burrows of freshwater insects, Freshw. Biol., 46(3), 317–327, 2001.

Wenzhofer, F. and Glud, R. N.: Small-scale spatial and temporal variability in coastal benthic O∼ 2 dynamics: Effects of fauna activity, Limnol. Oceanogr., 49, 1471–1481, 2004.

Wheatcroft, R. A., Jumars, P. A., Smith, C. R. and Nowell, A. R. M.: A mechanistic view of the particulate biodiffusion coefficient: step lengths, rest periods and transport directions, J. Mar. Res., 48(1), 177–207, 1990.

Wu, J., Jelinski, D. E., Luck, M. and Tueller, P. T.: Multiscale Analysis of Landscape Heterogeneity: Scale Variance and Pattern Metres, Geogr. Inf. Sci., 6(1), 6–19, doi:10.1080/10824000009480529, 2000.

Wu, J. and Li, H.: Concepts of scale and scaling, in Scaling and uncertainty analysis in ecology, pp. 3–15, Springer. [online] Available from: http://link.springer.com/content/pdf/10.1007/1-4020-4663-4_1.pdf (Accessed 22 September 2015), 2006.

Zhu, Q. and Aller, R. C.: A rapid response, planar fluorosensor for measuring two-dimensional pCO2 distributions and dynamics in marine sediments, Limnol. Oceanogr. Methods, 8, 326–336, doi:10.4319/lom.2010.8.326, 2010.

Zhu, Q. and Aller, R. C.: Two-dimensional dissolved ferrous iron distributions in marine sediments as revealed by a novel planar optical sensor, Mar. Chem., 136-137, 14–23, doi:10.1016/j.marchem.2012.04.002, 2012.

Zhu, Q., Aller, R. C. and Fan, Y.: Two-dimensional pH distributions and dynamics in bioturbated marine sediments, Geochim. Cosmochim. Acta, 70(19), 4933–4949, doi:10.1016/j.gca.2006.07.033, 2006.

Zorn, M. E., Lalonde, S. V., Gingras, M. K., Pemberton, S. G. and Konhauser, K. O.: Microscale oxygen distribution in various invertebrate burrow walls, Geobiology, 4(2), 137–145, doi:10.1111/j.1472-4669.2006.00074.x, 2006.

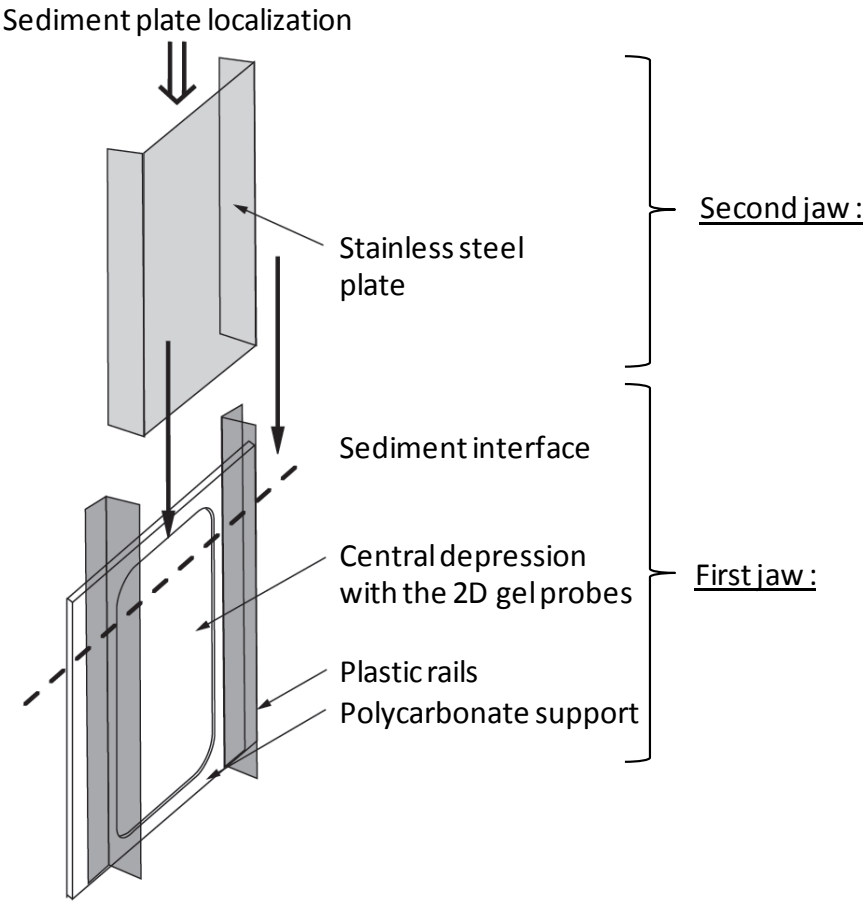

Figure 1 Schematic view of the "jaw device" for simultaneous sampling of sediment and porewater.

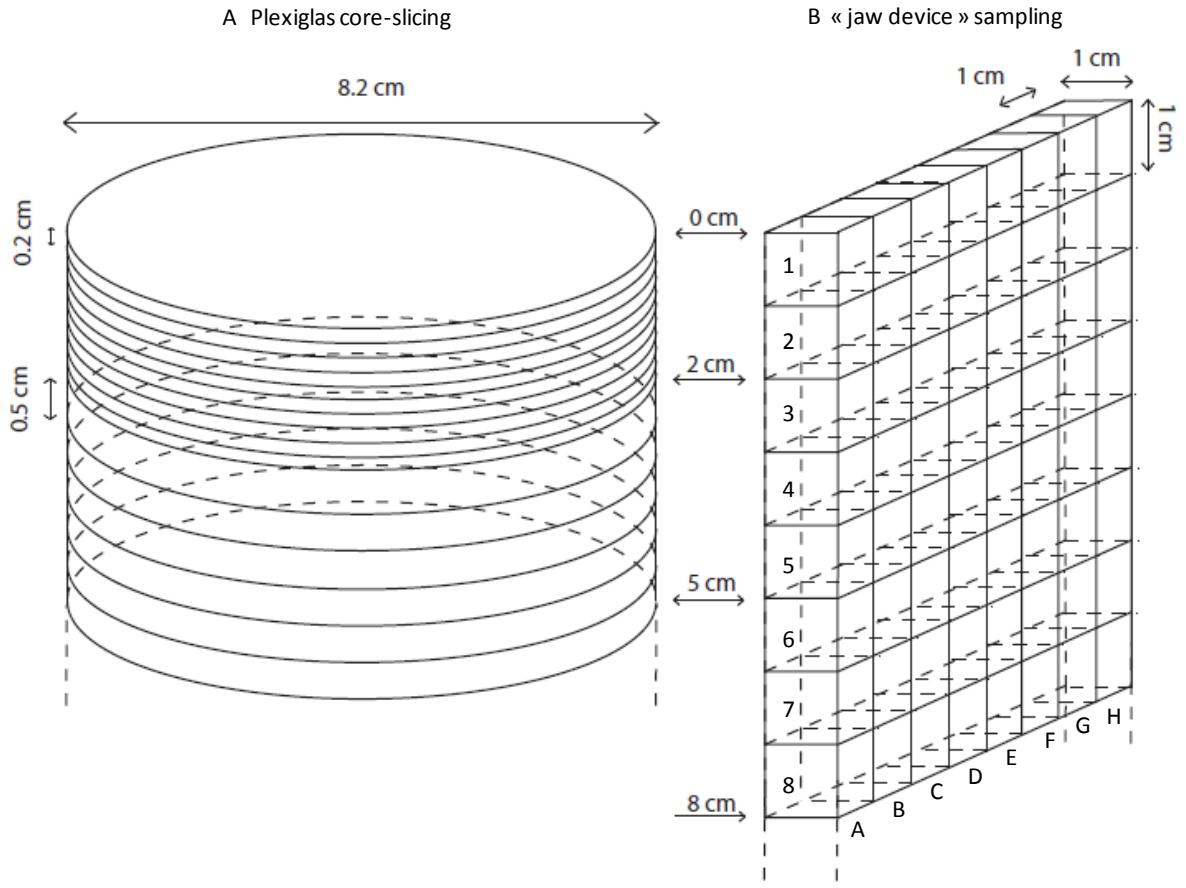

Figure 2. Sediment sampling methodology for living foraminiferal analyses. A: Usual 1D hand coring and layer slicing. B: Sediment plate sampling with the second jaw of the "jaw device" (Fig.1) and representation of the sediment cubic slicing.

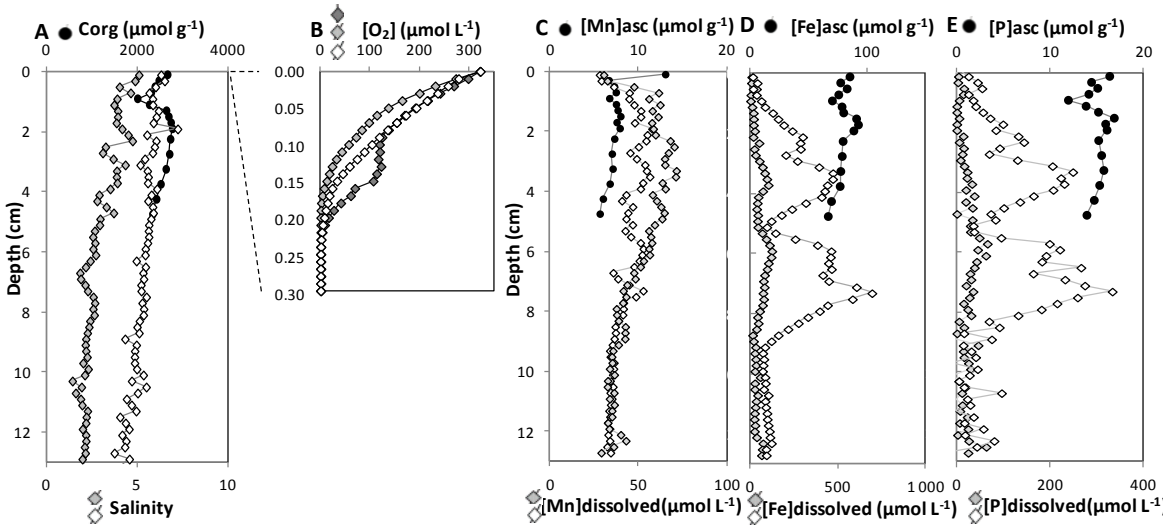

Figure 3: 1D geochemical features A- Vertical profile of total solid organic carbon (filled circles, uncertainty smaller than symbol size) and profiles of salinity (white and grey diamonds). B- Typical profiles of dissolved oxygen, the profile with dark grey diamonds is considered as bioturbated. C, D, E- Vertical profiles of manganese (C), iron (D) and phosphorus (E) in dissolved (white and gray diamonds for DET replicates) and reactive solid phase (ascorbate-leached) from the core (black circles).

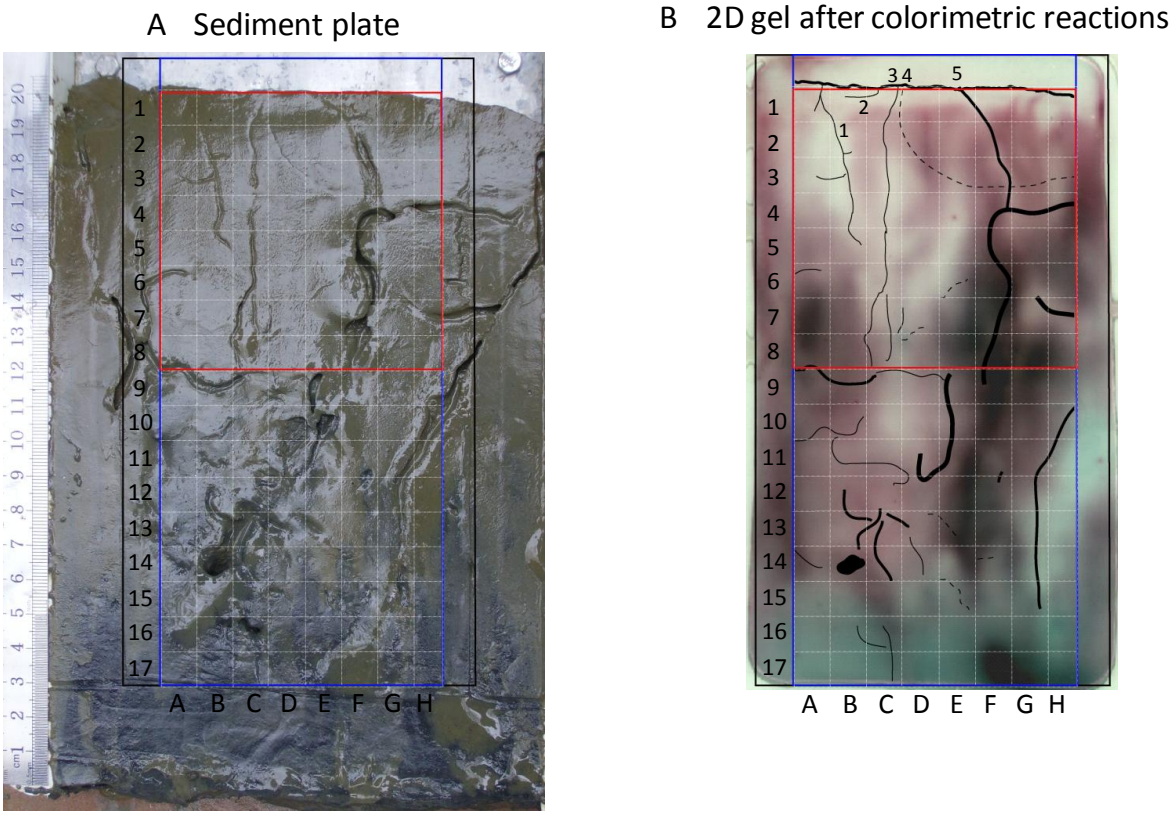

Figure 4: A - Picture of the sediment plate before cube slicing for foraminiferal analysis (sediment water interface at the top). B. Picture of the analyzed gel after colorimetric reactions: dissolved iron shown in dark pink and dissolved phosphorus in turquoise (burrows superimposed). The black rectangle corresponds to the gel limit, the blue rectangle to the limit of available dataset of dissolved iron and phosphorus and the red rectangle to the limit of the available dataset of foraminiferal distribution.

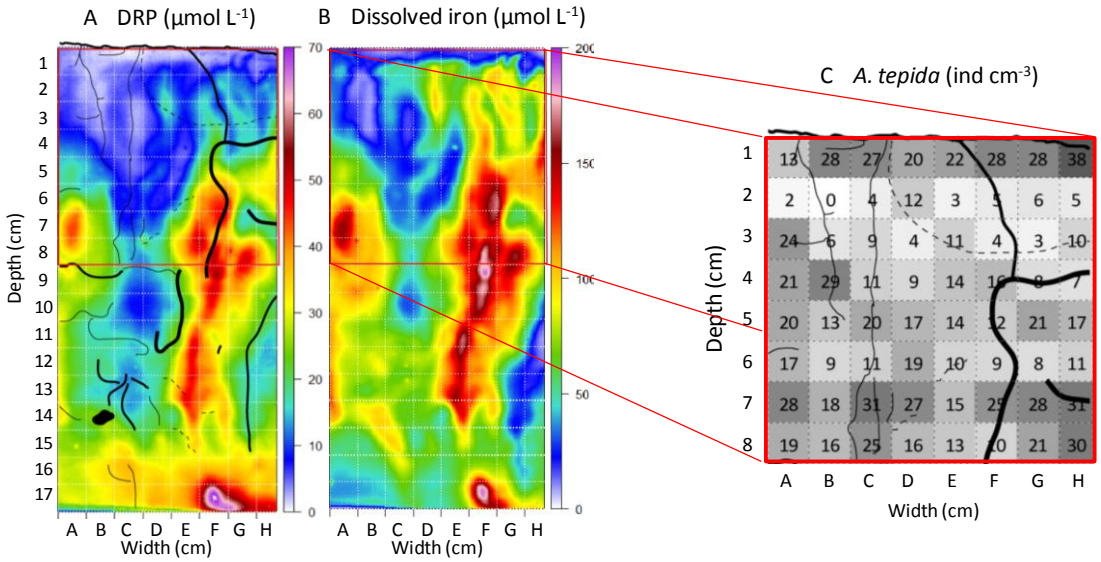

Figure 5: A B - Two dimensional concentrations after numerical analysis of dissolved reactive phosphorus (DRP) and dissolved iron. The distribution of burrows is shown on the DRP plot. Red lines represent the boundary of foraminiferal analysis. C - 2D distribution of *A. tepida* densities from the sediment plate with burrow distribution

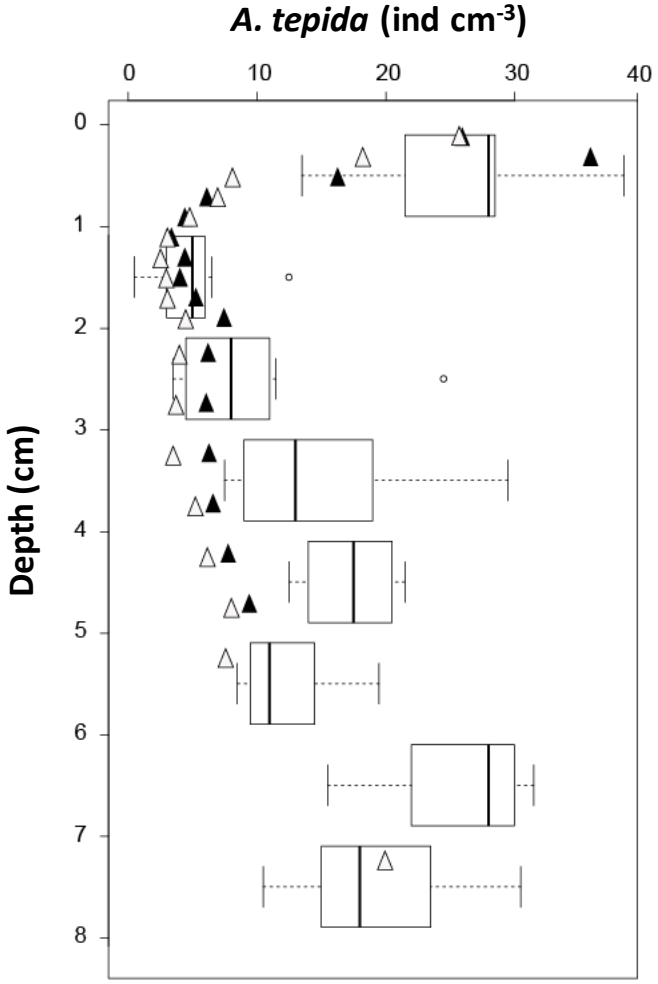

Figure 6: Vertical comparison of *A. tepida* densities from the 2 cores (full and open triangles) and the "jaw device" sampling (each boxplot represents the distribution of one layer; bars are first and third quartiles for the boxes length and whiskers are below 1.5 interquartiles; open circles are outliers).

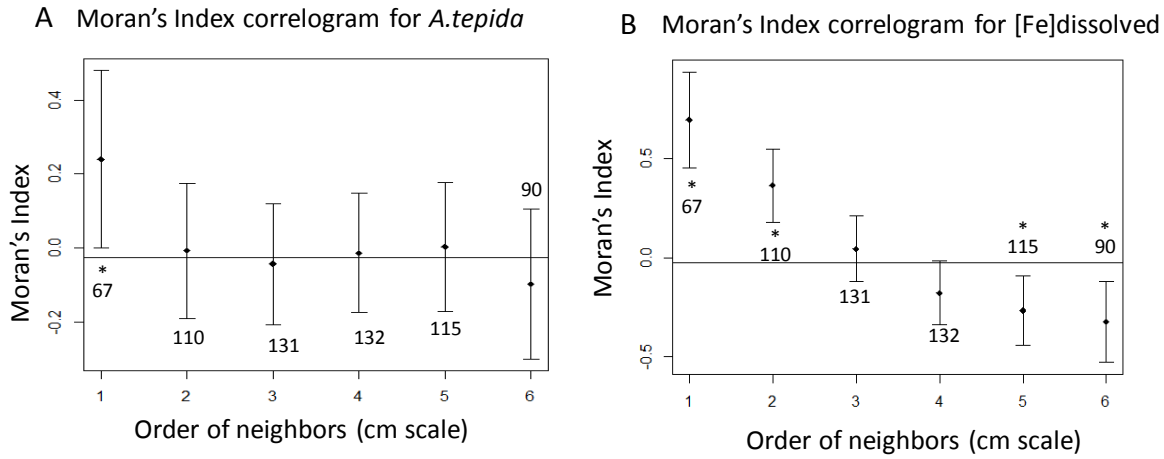

Figure 7: Moran's Index Correlograms for 3 to 8 cm depth: A- Moran's Index correlogram for *A. tepida* with a 1 cm resolution. B - Moran's Index correlogram for [Fe]dissolved with a 1 cm resolution. * shows significant differences from zero, error bars are twice the standard deviation; the numbers are the number of pairs for each order of neighbours.

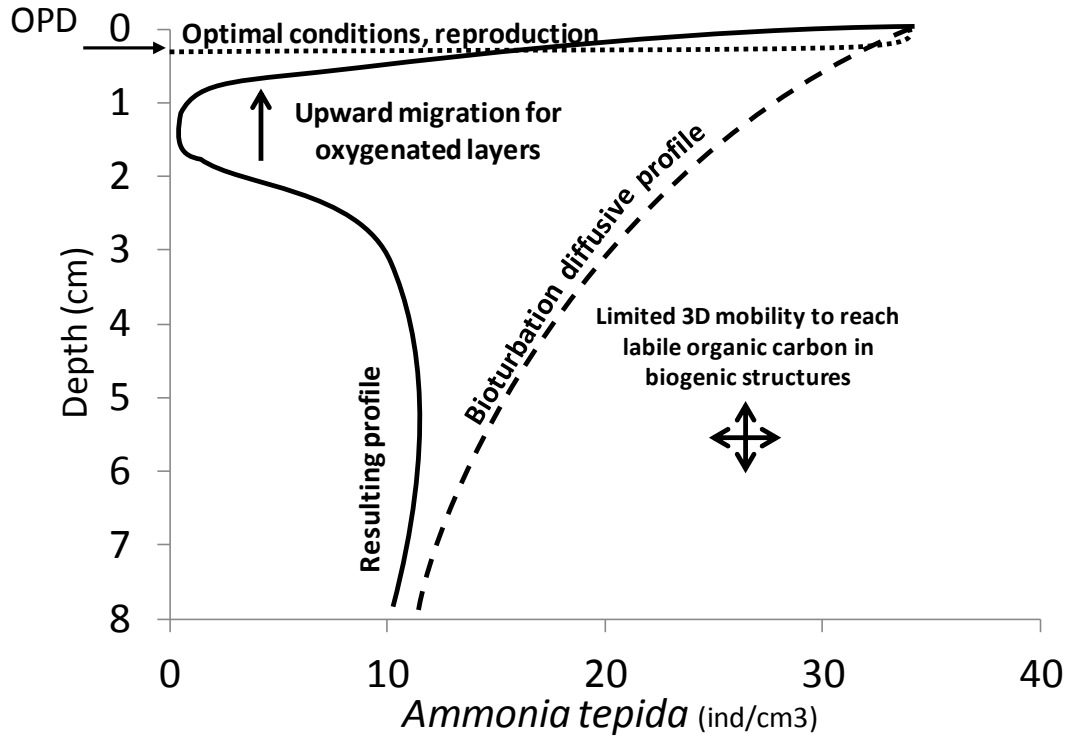

Figure 8: Putative mechanisms explaining the *A. tepida* density profile (OPD = Oxygen Penetration Depth).

1179